AD_____

GRANT NO: DAMD17-94-J-4120

TITLE: Ret Receptor: Functional Consequences of Oncogenic
Rearrangements

PRINCIPAL INVESTIGATOR(S):   Susan S. Taylor, Ph.D.

CONTRACTING ORGANIZATION: University of California, San Diego
                            La Jolla, California   92093-0934

REPORT DATE: October 1995

TYPE OF REPORT: Annual

PREPARED FOR: U.S. Army Medical Research and Materiel Command
                  Fort Detrick, Maryland   21702-5012
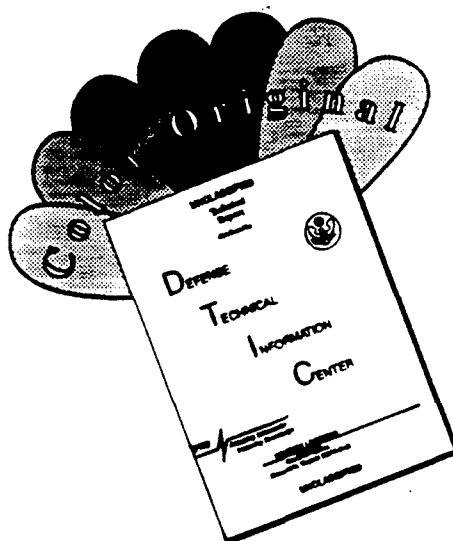
DISTRIBUTION STATEMENT: Approved for public release;
                          distribution unlimited

The views, opinions and/or findings contained in this report are
those of the author(s) and should not be construed as an official
Department of the Army position, policy or decision unless so
designated by other documentation.

DISCLAIMER NOTICE

THIS DOCUMENT IS BEST QUALITY AVAILABLE. THE COPY FURNISHED TO DTIC CONTAINED A SIGNIFICANT NUMBER OF COLOR PAGES WHICH DO NOT REPRODUCE LEGIBLY ON BLACK AND WHITE MICROFICHE.

REPORT DOCUMENTATION PAGE

Public reporting burden for this collection of information is estimated to average 1 hour per response, including the time for reviewing instructions, searching existing data sources, gathering and maintaining the data needed, and completing and reviewing the collection of information. Send comments regarding this burden estimate or any other aspect of this collection of information, including suggestions for reducing this burden. to Washington Headquarters Services, Directorate for Information Operations and Reports, 1215 Jefferson Davis Highway, Suite 1204, Arlington, VA 22202-4302, and to the Office of Management and Budget, Paperwork Reduction Project (0704-0188), Washington, DC 20503.

1. AGENCY USE ONLY (Leave blank)	2. REPORT DATE	3. REPORT TYPE AND DATES COVERED
	October 1995	Annual 15 Sep 94 – 14 Sep 95

4. TITLE AND SUBTITLE
Ret Receptor: Functional Consequences of Oncogenic Rearrangements

5. FUNDING NUMBERS
DAMD17-94-J-4120

6. AUTHOR(S)
Susan S. Taylor, Ph.D.

7. PERFORMING ORGANIZATION NAME(S) AND ADDRESS(ES)
University of California, San Diego
La Jolla, California 92093-0934

8. PERFORMING ORGANIZATION REPORT NUMBER

9. SPONSORING/MONITORING AGENCY NAME(S) AND ADDRESS(ES)
U.S. Army Medical Research and Materiel Command
Fort Detrick, Maryland 21702-5012

10. SPONSORING/MONITORING AGENCY REPORT NUMBER

11. SUPPLEMENTARY NOTES

12a. DISTRIBUTION/AVAILABILITY STATEMENT
Approved for public release; distribution unlimited

12b. DISTRIBUTION CODE

13. ABSTRACT (Maximum 200 words)

The overall goals of this proposal are to characterize the gene product of a novel oncogene *ret/ptc2*. This protein is a fusion of the RIα subunit of cAMP-dependent protein kinase and the kinase domain of a receptor tyrosine kinase. The ligand for the RET receptor is still unknown, however, this gene is associated with many inherited dominant cancers such as MEN2A, MEN2B, and Hirschprung's disease. *Ret/ptc2* is a constitutively active form of the RET receptor, and we believe it will be a prototype for other oncogene receptor tyrosine kinases. Our goals are to express large amounts of ret/ptc2 to establish the structural basis for its activation, to establish how the RET receptor functions *in vivo* by identifying the proteins it interacts with, and to model the ret kinase domain and map the sites of mutation that are known to be associated with various diseases. We are also constructing chimeras that resemble *ret/ptc2* using the kinase domains of the EGF receptor and the insulin receptor.

14. SUBJECT TERMS
Breast cancer, *ret/ptc2*, oncogenes, receptor tyrosine kinases, structure/function

15. NUMBER OF PAGES
27

16. PRICE CODE

17. SECURITY CLASSIFICATION OF REPORT	18. SECURITY CLASSIFICATION OF THIS PAGE	19. SECURITY CLASSIFICATION OF ABSTRACT	20. LIMITATION OF ABSTRACT
Unclassified	Unclassified	Unclassified	Unlimited

FOREWORD

Opinions, interpretations, conclusions and recommendations are those of the author and are not necessarily endorsed by the US Army.

_____ Where copyrighted material is quoted, permission has been obtained to use such material.

_____ Where material from documents designated for limited distribution is quoted, permission has been obtained to use the material.

_____ Citations of commercial organizations and trade names in this report do not constitute an official Department of Army endorsement or approval of the products or services of these organizations.

_____ In conducting research using animals, the investigator(s) adhered to the "Guide for the Care and Use of Laboratory Animals," prepared by the Committee on Care and Use of Laboratory Animals of the Institute of Laboratory Resources, National Research Council (NIH Publication No. 86-23, Revised 1985).

_____ For the protection of human subjects, the investigator(s) adhered to policies of applicable Federal Law 45 CFR 46.

_____ In conducting research utilizing recombinant DNA technology, the investigator(s) adhered to current guidelines promulgated by the National Institutes of Health.

_____ In the conduct of research utilizing recombinant DNA, the investigator(s) adhered to the NIH Guidelines for Research Involving Recombinant DNA Molecules.

_____ In the conduct of research involving hazardous organisms, the investigator(s) adhered to the CDC-NIH Guide for Biosafety in Microbiological and Biomedical Laboratories.   . . .

PI - Signature   Oct 13 1995   Date

TABLE OF CONTENTS

INTRODUCTION and BACKGROUND: Protein phosphorylation is probably the most important mechanism for regulation in eukaryotic cells. The tightly regulated enzymes that catalyze the phosphorylation of proteins, the protein kinases, are important components of signaling pathways that regulate normal cellular functions such as the cell cycle, metabolism, differentiation, memory and response to hormones, to name only a few. Over 400 are now known[1], and mutations that generate unregulated or constitutively activated protein kinases are typically oncogenic.

One of the simplest members of the protein kinase family is cAMP-dependent protein kinase, cAPK [2]. Being one of the best understood members of the protein kinase family, cAPK also serves as a template for the others since all of these enzymes have evolved from a common ancestor and contain a conserved catalytic core. cAPK, in the absence of cAMP, contains two types of subunits, a regulatory (R) subunit and a catalytic subunit (C). The R_2C_2 holoenzyme is catalytically inactive. In the presence of cAMP the complex dissociates into an R_2-(cAMP)$_4$ dimer and 2 free and active C-subunits. The crystal structure of the C-subunit, solved in our laboratory, serves as a structural template for the entire family of protein kinases [3]. It defines the folding of the polypeptide chain as well as the positions of the invariant residues that mostly cluster around the active site [4].

The objective of this grant is to characterize a novel oncogenic tyrosine kinase, Ret/ptc2, found in human papillary thyroid carcinomas. Specifically, we want to understand the molecular basis for its constitutive activation and the basis for its oncogenic properties. Ret/ptc2 is a rearranged gene product composed of the cAMP-dependent protein kinase (cAPK) regulatory subunit Iα (RIα) at its N-terminus fused to the tyrosine kinase core of the Ret proto-oncogene.

Ret Proto-Oncogene. The *ret* proto-oncogene (proto-*ret*) was cloned from a THP-1 human monocytic leukemia cDNA library, and is expressed in a number of human neuroblastoma and leukemia cell lines as 140-190 kDa glycoproteins [5]. Although its ligand is still unknown, sequence analysis identified it to be a member of the receptor tyrosine kinases. The putative extracellular domain contains Ca^{2+} binding domains similar to those in the cadherin proteins suggesting a role for proto-Ret in cell-cell recognition during development. *In situ* hybridization indicates that proto-*ret* expression is important for neurogenesis, and normal kidney organogenesis in the mouse [6; 7; 8] . Point mutations, premature truncations, and chromosomal rearrangements of human proto-*ret* with other genes have been linked to a number of human cancers.

The Ret Oncogene Family. The family of *ret* oncogenes can be divided into three separate classes. The first class of *ret* oncogenes was produced *in vitro* by transfecting NIH 3T3 cells with high molecular weight DNA from human cell lymphomas [9], human colon carcinoma [10], and human stomach cancer tissue [11]. The high propensity of *proto-ret* to rearrange with other genes is reflected in its name for _re_arranged upon _t_ransfection [9].

The second class consists of missense mutations and truncated forms of proto-*ret* that are proposed to result in either hyper- or hypoactivity. These are associated with three dominantly inheirited human cancer syndromes: MEN 2A,

MEN 2B, familial medullary thyroid carcinoma (FMTC) [12; 13], and Hirschsprung's disease [14; 15]. Germ-line mutations of proto-*ret* are dominant and are associated specifically with MEN 2A [16].

The third class of *ret* oncogenes, isolated from human papillary thyroid carcinomas [17]; Bongarzone; 1993 #2580; Grieco, 1994 #2892; Bongarzone, 1994 #2893, consists of 3 types: *ret/ptc1*, *ret/ptc2* and *ret/ptc3*. The 5' end of the each oncogene is a portion of an unrelated gene fused in frame to the identical splice site of the proto-*ret* gene resulting in an intact functional Ret kinase.

The *ret/ptc1* and *ret/ptc2* oncogenes each produce 2 isoforms as a result of alternative splicing, and unlike proto-Ret are completely cytosolic, phosphorylated on tyrosine residues, and constitutively active [18]. The 5' end of *ret/ptc1* is a fragment of a new gene designated, H4(DS10S170) [19; 20], and the 5' end of *ret/ptc3* encodes a gene designated *ele1* or ret fused gene, whose gene product does not show sequence identity to known proteins [21; 22; 23]. Unlike *ret/ptc1* and *ret/ptc3*, the N-terminal sequence of *ret/ptc2* gene [18] encodes approximately 60% of a biochemically well characterized protein, the RIα subunit of cAPK. Comparison of proto-Ret, the cAPK RIα-subunit, and Ret/ptc2 genes is illustrated in Figure 1.
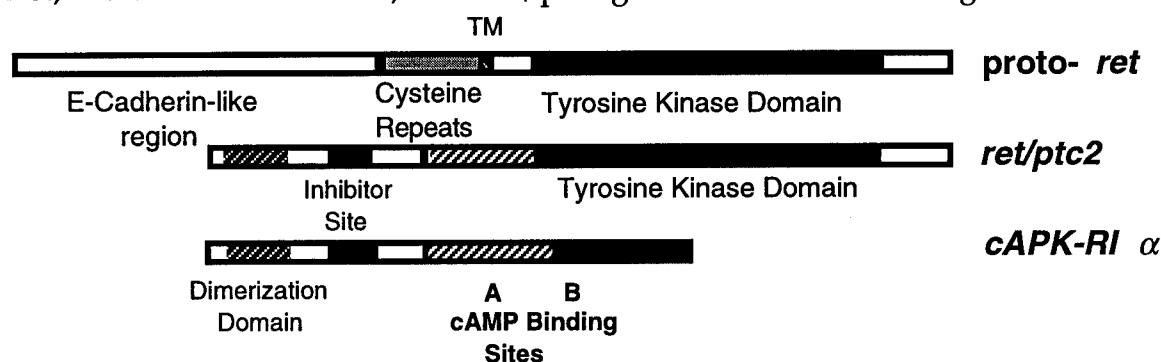

Figure 1. Comparison of *proto-ret*, *ret/ptc2*, and *cAPK RIα subunit*

Regulatory Subunit of cAPK. The regulatory subunit of cAPK maintains the C subunit in an inactive state by forming a stable R_2C_2 tetramer. A pseudo-substrate inhibition sequence in the R-subunit mimics peptide substrates and fills the peptide binding site of the C-subunit. The binding of cAMP to R causes the complex to dissociate and to release two active C-subunits.

Although there are several unique gene products in the R-subunit family, all share a well-defined domain structure. The RIα subunit begins with a dimerization domain close to its amino terminus followed by a pseudo-substrate inhibitory region and ends with two tandem cAMP binding domains. The RIα dimerization domain is stabilized by two antiparallel interchain disulfide bonds [24]. Circular dichoism studies of the proteolytically isolated RIα dimerization domain indicate it is predominantly α-helical, and extremely stable to thermal denaturation [25]. The crystal structure of the bovine RIα was recently solved in our laboratory [26]. The splice site of the RIα fragment in Ret/ptc2 is at the beginning of the αC-A helix, thus

3

deleting the last 21% of the A site cAMP-binding domain and the entire B-site cAMP binding domain.

SPECIFIC AIMS

Our overall long terms goals are to understand the molecular basis for the constitutive activation of ret/ptc2 and to characterize the physiological functioning of both *ret/ptc2* and proto-*ret*. Our specific aims are the following:

1.   To understand the structural features of ret/ptc2 that are required for its oncogenic properties. To achieve this we have developed an *in vivo* assay to measure a mitogenic response of *ret/ptc2* by microinjecting it into the nucleus of rat fibroblast $10T^1/_2$ cells.

2.   To characterize the biochemical properties of *ret/ptc2* by overexpressing the protein in *E. coli* and human kidney 293 cells. Phosphorylation sites will be mapped and kinetic properties characterized.

3.   To identify *Ret/ptc2* binding proteins identify using a yeast two-hybrid system.

4.   To construct homologs of *ret/ptc2* using the tyrosine kinase domains of the EGF receptor and the insulin receptor.

5.   To model the kinase core of *Ret/ptc2* based on the crystal structure of the C-subunit of cAPK and on the kinase domain of the insulin receptor.

We have made excellent progress in each of these areas, as indicated below, during this first year of the grant. Because much of this work is still unpublished, we shall describe it in some detail. This is an entirely new project for our laboratory but it is quickly becoming a major focus.

RESEARCH DESIGN AND EXPERIMENTAL RESULTS

Expression and Purification of Ret/ptc2: We have succeeded in expressing the 76 kDa isoform of *Ret/ptc2* both in *E. coli* and in human kidney 293 cultured cells. In the bacterial expression system, *ret/ptc2* was inserted behind a hexahistidine sequence in the bacterial expression vector, pET15b (Novagen), and transformed into the host strain, NovaBlue(DE3). Yields are 1-2 milligrams per liter.

Ret/ptc2 is detected with a polyclonal rabbit antipeptide antibody to residues 535-551 in the kinase domain. Recombinant r*Ret/ptc2* is soluble, stable and is recognized by both the C-terminal Ret peptide antibody and a monoclonal mouse phosphotyrosine antibody. Substitution of the bovine RIα sequence for the human RIα sequence in *Ret/ptc2* results in increased levels of expression. Expression of *Ret/ptc2* both in *E.coli* and in human kidney 293 cells yields a gene product which is multiply phosphorylated on tyrosine residues.

His_6-r*Ret/ptc2* was purified by affinity chromatography using a nickel resin (Fig. 2, panel A, lane 3). *Ret/ptc2* autophosphorylates *in vitro*, and labeling with [γ-^{32}P]-ATP is 2-3x higher in the presence of Mn^{+2} than Mg^{+2}. Autophosphorylation of *Ret/ptc2* results in a molecular weight shift of the major band (Fig. 2, panel A, compare lanes 2 and 3). Autoradiography of autophosphorylated *Ret/ptc2* in Fig. 2, reveals 5 labeled protein bands (Fig. 2, panel B, lane 2) suggesting multiple

4

phosphorylation sites. The phosphorylated *Ret/ptc2* isoforms observed in Figure 2, panel A, lanes 2 & 3 are all recognized by the C-terminal Ret peptide antibody and the antiphosphotyrosine antibody. Preliminary results from inhibition assays indicate that both the cAPK C-subunit and cAMP bind to *Ret/ptc2*.
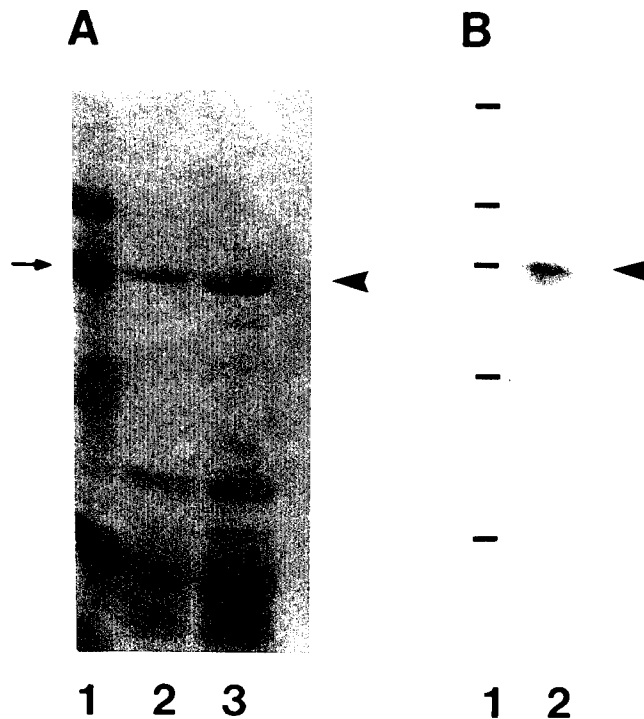

Figure 2. Purified SDS-PAGE separated His_6-Ret/ptc2, electroblotted onto PVDF membrane, and stained with Ponceau S. Panel A: lane 1, molecular weight standars, lane 2: autophosphorylated [^{32}P]-His_6-Ret/ptc2, lane 3: purified His_6-Ret/ptc2. The arrow on the left identifies the 74.25 kDa pre-stained bovine serum albumin molecular weight standard, and the arrowhead identifies His_6-Ret/ptc2. Panel B: lane 1: molecular weight standards, lane 2: autoradiography of autophosphorylated [^{32}P]-His_6-Ret/ptc2 from Panel A, lane 2. The arrowhead points to the phosphorylated His_6-Ret/ptc2 isoforms.

Biological Assay of Ret/ptc2 Mutants: Microinjection of *ret/ptc2* and mutants of *ret/ptc2* has provided us with an *in vivo* assay by which the induction of DNA synthesis by Ret/ptc2 and mutants can be qualitatively evaluated. Developing this *in vivo* assay for the mitogenic effects of *ret/ptc2* was a critical step. In this assay, *ret/ptc2* was inserted into the mammalian expression vector, pRc/CMV (Invitrogen), behind the human cytomegalovirus promoter and microinjected into rat fibroblast cells ($10T^1/_2$). Injected cells are visualized by fluorescence, and DNA synthesis is measured by the incorporation of 5-bromo-deoxyuridine [27]. The loss of mitogenic activity of inactive Ret/ptc2 mutants is not attributable to the inability of the cells to express these proteins since similar levels of protein expression were

5

visualized in all injected cells by immunofluorescence. With this system we have established: a) Ret/ptc2 requires only the RIα dimerization domain to induce DNA synthesis, b) site-specific mutations in Ret/ptc2 of kinase domain residues corresponding to the MEN 2B and Hirschsprung's disease mutations yield results similar that observed in the human disease phenotypes, c) selective mutation of Tyr350, Tyr424, Tyr505,Tyr586 to Phe show reduced levels or loss of DNA synthesis, d) substitution of the bovine RIα gene for the human RIα gene in *ret/ptc2* does not affect its ability to induce DNA synthesis [27].

The Ret/ptc2 Hirschsprung's disease mutants did not induce DNA synthesis whereas the MEN 2B mutant elicited a mitogenic response. These results are consistent with the human Ret oncogene disease phenotypes whereby Hirschsprung's disease is presumed to be due to loss of function, and the MEN 2B mutation has been proposed to elicit an altered substrate specificity such that inappropriate mitogenic signaling pathways are activated [28; 29]. Recent identification of two other Ret kinase domain mutants associated with FMTC, Glu768Asp [30], and Val804Leu [31], which correspond to residues Glu292 and Val328 in *Ret/ptc2*, respectively, are now being introduced into the *Ret/ptc2* kinase domain and tested in our *in vivo* microinjection assay. Glu292 resides above the glycine loop in our Ret/ptc2 model. The Val328 residue in our Ret/ptc2 model resides at the end of β-strand 5 in the small lobe, approximately 5 residues from the hinge region which separates the small and large lobes. Mutation of this residue from Val to Leu shortens the distance of this residue to within 3 A of Leu303, which is located on the αC-helix in the small lobe. Val328 corresponds to Met120 in the cAPK C-subunit. Met120 is one of several residues which interacts with the adenine ring of ATP via hydrophobic interactions and hydrogen bonding [32]. Kinetic analysis of all the Ret/ptc2 missense mutants will define their catalytic efficiencies and elucidate the molecular basis of their disease phenotypes.

Mutations of Tyr350 and Tyr424 to Phe decreased the mitogenic response in our assay [27]. Tyr350 resides within an insert sequence in the PDGF kinase domain which contains two SH2 binding sites, and thus this phosphorylated residue may be involved in downstream signaling. Phosphorylation of Tyr424, corresponding to Tyr1158 in the InsR, is necessary for full InsR activity [33]. Mutation of Tyr429, which corresponds to Thr197 in the cAPK C-subunit, Tyr416 in *src*, and Tyr1163 in the InsR [34], did not result in the induction of DNA synthesis. This result suggests the activation of the Ret/ptc2 kinase domain is unlike that of the *src*, a cytosolic tyrosine kinases, and the Ser/Thr kinase, cAPK. In addition, this result indicates that phosphorylation of specific tyrosyl residues which serve to activate recepor tyrosine kinases (RTKs) differ amongst the RTKs. Molecular modeling studies of the Ret/ptc2 kinase core indicate Tyr586 resides at an exposed site of the proposed structure, whereas Tyr505 is less exposed albeit highly conserved in other RTKs which suggests it may be important for structural stability.

Phosphorylation of Tyr350 and Tyr586 *in vivo*, may provide docking sites for SH2 containing proteins. Immunoprecipitation of both Ret/ptc1 and Ret/ptc2 expressed in NIH 3T3 cells have shown that phosphorylated Shc is associated with all four isoforms of the 2 proteins [35]. *In vitro* binding assays of cell lysates to

immobilized glutathione-fused Grb2 or Grb2 SH2 domains indicate the SH2 domains of Grb2 may also be associated with the anti-Shc immunoprecipitated Ret/ptc1 and Ret/ptc2 isoforms as well as other phosphorylated unidentified proteins [35]. The reduction or loss of mitogenic activity in the Ret/ptc2 tyrosine mutants may stem from effects of structural instability, alterations in catalytic activity, or decreased interactions with downstream signaling proteins. Further investigation of these Ret/ptc2 tyrosine mutants is underway.

Yeast Two Hybrid System: We have begun to use the yeast two hybrid system to isolate RET-binding proteins. Using *ret/ptc2* as the bait, we have been able to identify several proteins that specifically bind to the RET portion of *ret/ptc2*. These proteins are now being expressed as fusion proteins and binding is being confirmed *in vitro*. Several of these proteins contain SH2 domains and, using a series of Tyr/Phe mutants, the binding of each of these proteins is being correlated with a specific tyrosine residue. The effect of each of these proteins in the in vivo assay is simultaneously being tested. From these studies is emerging a comprehensive set of RBP's (Ret Binding Proteins) that dock at specific sites along the polypeptide chain. Binding is being confirmed by surface plasmon resonance using the expressed protein and the expressed and purified binding domains.

Identification of Phosphorylated Tyrosine Residues: To identify the phosphorylation sites in *Ret/ptc2*, we are labelling the protein *in vivo* with [^{32}Pi]. Western analysis of SDS-PAGE separated His$_6$-Ret/ptc2 indicates it is multiply phosphorylated on tyrosine residues. Two dimensional peptide maps will be used to identify ^{32}P-labelled peptides. Peptides will also be separated by reverse-phase HPLC, and the [^{32}P]-peptide(s) will be sequenced. The phosphorylation sites in the recombinant *ret/ptc2* will then be compared with the sites that are labeled when *ret/ptc2* is explressed in eukaryotic cells to make certain that the sites are the same. Phosphaorylation sites will also be indentified by electrospray mass spectrometry.

Identification of phosphorylated tyrosine residues in *Ret/ptc2* will enable us to design and synthesize an optimum consensus peptide substrate for use as a Ret/ptc2-specific peptide substrate. By identifying a consensus peptide based on the autophosphorylation sequences, we expect to gain a higher specific activity and thus a greater sensitivity in our *in vitro* assay.

An enzymatic assay for *Ret/ptc2*, based on a modification of the autophoshorylation assay whereby the [^{32}P]-phosphorylated peptide substrate is bound to a phosphocellulose membrane disk for quantitation by liquid scintillation counting, is now being established for routine use. Steady state parameters such as K_m, K_{cat} and V_{max} will be determined from plots of initial velocity versus substrate concentration. This kinetic analysis will be essential for quantifying the specific effects of the various mutations as well as for under-standing, in general, the biological properties of this enzyme.

Modelling of the Ret Tyrosine Kinase Domain: The *ret* kinase domain has been modeled based on the structure of the catalytic subunit of cAPK and the recently solved structures of the insulin receptor kinase [36]. We are done mapping the sites that are associated with the various malignancies. By mapping these sites and correlating the sites with the phenotype displayed by the malignancy, we hope to better understand *ret/ptc2* as well as proto-*ret* functions.

7

CONCLUSION

This represents a totally new project for my laboratory, and the progress during this first year has been excellent. With the biological assay we have been able to establish what is essential for the mitogenic properties of *ret/ptc2*. In conjunction with this, we are now using the yeast two-hybrid system to identify Ret binding proteins and are developing a comprehensive picture of this receptor tyrosine kinase and its *in vivo* partners. At the same time we have developed an *E. coli* expression system that yields mg quantities of proteins both for *Ret/ptc2* and for the EGF and insulin receptor homologs. Finally, we have been modeling the kinase portion of Ret based on our structure of the cAPK C-subunit and of the crystal structure of the insulin receptor kinase domain. Of particular importance now is mapping of the various mutation sites in Ret that are known to be linked with a wide variety of malignancies.

REFERENCES

1. Hanks, S.K., & Hunter, T. Protein kinases 6. The eukaryotic protein kinase superfamily: kinase (catalytic) domain structure and classification. *Faseb J.* **9** (8), 576-596 (1995).

2. Taylor, S.S.,Buechler, J.A., & Yonemoto, W. cAMP-dependent Protein Kinase: Framework for a Diverse Family of Regulatory Enzymes. *Annu. Rev. Biochem.* **59** 971-1005 (1990).

3. Knighton, D.R.,Zheng, J.,Ten Eyck, L.F.,Ashford, V.A.,Xuong, N.-h.,Taylor, S.S., & Sowadski, J.M. Crystal Structure of the Catalytic Subunit of cAMP-dependent Protein Kinase. *Science* **253** 407-414 (1991).

4. Taylor, S.S.,Knighton, D.R.,Zheng, J.,Ten Eyck, L.F., & Sowadski, J.M. Structural Framework for the Protein Kinase Family. *Annu. Rev. Cell Biol.* **8** 429-462 (1992).

5. Takahashi, M.,Buma, Y., & Taniguchi, M. Identification of the *ret* proto-oncogene in neuroblastoma and leukemia cells. *Oncogene* **6** 297-301 (1991).

6. Pachis, V.,Mankoo, B., & Constantini, F. Expression of the c-ret proto-oncogene during mouse embryogenesis. *Development* **119** 1005-17 (1993).

7. Sugaya, R.,Ishimaru, S.,Hosoya, T.,Saigo, K., & Emori, Y. A Dropsophila homolog of human proto-oncogene ret transiently expressed in embryonic meuronal precursor cells including neuroblasts and CNS cells. *Mech. Dev.* **45** 139-45 (1994).

8. Schuchardt, A.,D'Agati, V.,Larsson, B.L.,Constantini, F., & Pachnis, V. Defects in the kidney and enteric nervous system of mice lacking the tyrosine kinase receptor Ret [see comments]. *Nature* **367** 380-3 (1994).

9. Takahashi, M.,Ritz, J., & Cooper, G.M.   Activation of a Novel Human
Transforming Gene, *ret*, by DNA Rearrangement. *Cell* **42** 581-588 (1985).

10. Ishizaka, Y.,Tahira, T.,Ochiai, M.,Ikeda, I.,Sugimura, T., & Nagao, M. Molecular
Cloning and Characterization of Human ret-II Oncogene. *Oncogene Res.* **3** 193-7
(1988).

11. Kunieda, T.,Marsui, M.,Nomura, N., & Ishizaki, R. Cloning of an Activated
Human ret Gene With a Novel 5' Sequence Fused by DNA Rearrangement. *Gene*
107 323-8 (1991).

12. Hofstra, R.M.,Landsvater, R.M.,Ceccherini, I.,Stulp, R.P.,Stelwagen, T.,Luo,
Y.,Pasini, B.,Hoppener, J.W.M.,Ploos van Amstel, H.K.,Romeo, G.,Lips, C.J.M., &
Buys, C.C.C.M. A mutation in the RET proto-oncogene associated with multiple
endocrine neoplasia type 2B and sporadic medullary thyroid carcinoma. *Nature* **367**
375-376 (1994).

13. Mulligan, L.M.,Eng, C.,Healey, C.S.,Clayton, D.,Kwok, J.B.,Gardner, E.,Ponder,
M.A.,Frilling, A.,Jackson, C.E., & Lehnert, H. Specific mutations of the RET proto-
oncogene are related to disease phenotype in MEN 2A and FMTC. *Nat. Gent.* **6** 70-4
(1994).

14. Edery, P.,Lyonney, S.,Mulligan, L.M.,Pelet, A.,Dow, E.,Abel, L.,Holder, S., &
Nihoul. Mutations of the RET proto-oncogene in Hirschsprung's disease. *Nature*
367 378-80 (1994).

15. Romeo, G.,Ronchetto, P.,Luo, Y.,Barone, V.,Seri, M.,Ceccherini, I.,Pasini,
B.,Bocciardi, R.,Lerone, M., & Kaarianinen, H. Point mutations affecting the
tyrosine kinase domain of the RET proto-oncogene in Hirschsprung's disease.
Nature **367** 377-8 (1994).

16. Mulligan, L.M.,Kwok, J.B.J.,Healey, C.S.,Elsdon, M.J.,Eng, C.,Gardner, E.,Love,
D.R.,Mole, S.E.,Moore, J.K.,Papi, L.,Ponder, M.A.,Telenius, H.,Tunnacliffe, A., &
Ponder, B.A.J. Germ-Line Mutations of the RET Proto-Oncogene in Multiple
Endocrine Neoplasia Type 2A. *Nature* **363** 458-460 (1993).

17. Grieco, M.,Santoro, M.,Berlingieri, M.T.,Melillo, R.M.,Donghi, R.,Bongarzone,
I.,Pierotti, M.A.,Della Porta, G.,Fusco, A., & Vecchio, G. PTC is a novel rearranged
form of the ret proto-oncogene and is frequently detected *in vivo* in human thyroid
papillary carcinomas. *Cell* **60** 557-563 (1990).

18. Bongarzone, I.,Monzini, N.,Borrello, M.G.,Carcano, C.,Ferraresi, G.,Arighi,
E.,Mondellini, P.,Della Porta, G., & Pierotti, M.A. Molecular characterization of a
thyroid tumor-specific transforming sequence formed by the fusion of ret tyrosine

kinase and the regulatory subunit RI alpha of cyclic AMP-dependent protein kinase A. *Mol. Cell. Biol.* **13** 358-366 (1993).

19. Grieco, M.,Cerrato, A.,Santoro, M.,Fusco, A.,Melillo, R.M., & Vecchio, G. Cloning and characterization of H4 (D10S170), a gene involved in RET rearrangements in vivo. *Oncogene* **9** 2531-5 (1994).

20. Tong, Q.,Li, Y.,Smanik, P.A.,Fithian, L.J.,Xing, S.,Mazzaferri, E.L., & Jhiang, S.M. Characterization of the promoter region and oligomerization domain of H4 (D10S170), a gene frquently rearranged with the ret proto-oncogene. *Oncogene* **10** 1781-7 (1995).

21. Bongarzone, I.,Butti, M.G.,Coronelli, S.,Borello, M.G.,Santoro, M.,Mondellini, P.,Pilotti, S.,Fusco, A.,Della, P.G., & Pierotti, M.A. Frequent activation of ret proto-oncogene by fusion with a new activating gene in papillary thyroid carcinomas. *Cancer Res.* **54** 2879-85 (1994).

22. Santoro, M.,Dathan, N.A.,Berlingieri, M.T.,Bongarzone, I.,Paulin, C.,Grieco, M.,Pierotti, M.A.,Vecchio, G., & Fusco, A. Molecular characterization of RET/PTC3; a novel rearranged version of the RET proto-oncogene in a human thyroid papillary carcinoma. *Oncogene* **9** 509-16 (1994).

23. Minoletti, F.,Butti, M.G.,Coronelli, S.,Miozzo, M.,Sozzi, G.,Pilotti, S.,Tunnacliffe, A.,Poerotti, M.A., & Bongarzone, I. The two genes generating RET/PTC3 are localized in chromosomal band 10q11.2. *Genes, Chromosomes and Cancer* **11** 51-7 (1994).

24. Bubis, J.,Vedvick, T.S., & Taylor, S.S. Antiparallel Alignment of the Two Protomers of the Regulatory Subunits of the Regulatory Subunit Dimer of cAMP-Dependent Protein Kinase I. *J. Biol. Chem.* **262** 14961-14966 (1987).

25. León, D.,Herberg, F.W.,Banky, P., & Taylor, S.S. Characterization of an α- Helical Dimer from the Regulatory Subunit of cAMP-Dependent Protein Kinase. (Submitted 1995).

26. Su, Y.,Dostmann, W.R.G.,Herberg, F.W.,Durick, K.,Xuong, N.-h.,Ten Eyck, L.F.,Taylor, S.S., & Varughese, K.I. Regulatory (RIα) Subunit of cAMP-dependent Protein Kinase: Crystal Structure of a 1-91 Deletion Mutant Defines Cooperative cAMP Binding Sites. *In press Science* (1995).

27. Durick, K.,Yao, V.J.,Borrello, M.G.,Bongarzone, I.,Pierotti, M.A., & Taylor, S.S. Tyrosines outside the kinase core and dimerization are required for the mitogenic activity of RET/ptc2. *in press J. Biol. Chem.* (1995).

28. Songyang, Z.,Carraway, K.L.,Eck, M.J.,Harrison, S.C.,Feldman, R.A.,Mohammedi, M.,Schlessinger, J.,Hubbard, S.R.,Smith, D.P.,Eng, C.,Lorenzo,

M.J.,Ponder, B.A.J.,Mayer, B.J., & Cantley, L.C. Catalytic specificity of protein-tyrosine kinases is critical for selctive signalling. *Nature* **373** 536-9 (1995).

29. Santoro, M.,Carlomagno, F.,Romano, A.,Bottaro, D.P.,Dathan, N.A.,Grieco, M.,Fusco, A.,Vecchio, G.,Matoskova, B.,Kraus, M.H., & DiFiore, P.P. Activation of RET as a dominant transforming gene by germline mutations of MEN2A and MEN2B. *Science* **267** 381-3 (1995).

30. Eng, C.,Smith, D.P.,Mulligan, L.M.,Healey, C.S.,Zvelebil, M.J.,Stonehouse, T.J.,Ponder, M.A.,Jackson, C.E.,Waterfield, M.D., & Ponder, B.A.J. A novel point mutation in the tyrosine kinase domain of the RET proto-oncogene in sporadic medullary thyroid carcinoma and in a family with FMTC. *Oncogene* **10** 509-13 (1995).

31. Bolino, A.,Schuffenecker, I.,Luo, Y.,Seri, M.,Silengo, M.,Tocco, T.,Chabrier, G.,Houdent, C.,Murat, A.,Schlumberger, M.,Tourniaire, J.,Lenoir, G.M., & Romeo, G. RET mutations in exons 13 and 14 of FMTC patients. *Oncogene* **10** 2415-19 (1995).

32. Zheng, J.,Knighton, D.R.,Ten Eyck, L.F.,Karlsson, R.,Xuong, N.-h.,Taylor, S.S., & Sowadski, J.M. Crystal Structure of the Catalytic Subunit of cAMP-dependent Protein Kinase Complexed with MgATP and Peptide Inhibitor. *Biochemistry* **32** (9), 2154-2161 (1993).

33. White, M.,Shoelson, S.,Keutmann, H., & Kahn, C. A cascade of tyrosine autophosphorylations in the beta-subunit activates the phosphotransferase of the insulin receptor. *J. Biol. Chem.* **263** 2969-80 (1988).

34. Hanks, S.K.,Quinn, A.M., & Hunter, T. The Protein Kinase Family: Conserved Features and Deduced Phylogeny of the Catalytic Domains. *Science* **241** 42-52 (1988).

35. Borrello, M.G.,Pelicci, G.,Arighi, E.,De, F.L.,Greco, A.,Bongarzone, I.,Rizzetti, M.,Pelicci, P.G., & Pierotti, M.A. The oncogenic versions of the Ret and Trk tyrosine kinases bind Shc and Grb2 adaptor proteins. *Oncogene* **9** 1661-8 (1994).

36. Hubbard, S.R.,Wei, L.,Ellis, L., & Hendrickson, W.A. Crystal structure of the tyrosine kinase domain of the human insulin receptor [see comments]. *Nature* **372** (6508), 746-754 (1994).

APPENDIX

1. Su, Y.,Dostmann, W.R.G.,Herberg, F.W.,Durick, K.,Xuong, N.-h.,Ten Eyck, L.F.,Taylor, S.S., & Varughese, K.I. Regulatory (RIα) Subunit of cAMP-dependent Protein Kinase: Crystal Structure of a 1-91 Deletion Mutant Defines Cooperative cAMP Binding Sites. *In press Science* (1995).

2. Durick, K.,Yao, V.J.,Borrello, M.G.,Bongarzone, I.,Pierotti, M.A., & Taylor, S.S. Tyrosines outside the kinase core and dimerization are required for the mitogenic activity of RET/ptc2. *J. Biol. Chem.* In Press (1995).

SCiENCE

Regulatory Subunit of Protein Kinase A: Structure of Deletion Mutant with cAMP Binding Domains

Y. Su, W. R. G. Dostmann,* F. W. Herberg,† K. Durick,
N-h. Xuong, L. Ten Eyck, S. S. Taylor, and K. I. Varughese

Regulatory Subunit of Protein Kinase A: Structure of Deletion Mutant with cAMP Binding Domains

Y. Su, W. R. G. Dostmann,* F. W. Herberg,† K. Durick, N-h. Xuong, L. Ten Eyck, S. S. Taylor,‡ K. I. Varughese

In the molecular scheme of living organisms, adenosine 3′,5′-monophosphate (cyclic AMP or cAMP) has been a universal second messenger. In eukaryotic cells, the primary receptors for cAMP are the regulatory subunits of cAMP-dependent protein kinase. The crystal structure of a 1–91 deletion mutant of the type Iα regulatory subunit was refined to 2.8 Å resolution. Each of the two tandem cAMP binding domains provides an extensive network of hydrogen bonds that buries the cyclic phosphate and the ribose between two β strands that are linked by a short α helix. Each adenine base stacks against an aromatic ring that lies outside the β barrel. This structure provides a molecular basis for understanding how cAMP binds cooperatively to its receptor protein, thus mediating activation of the kinase.

$\mathbf{P}$rotein phosphorylation and dephosphorylation is one of the principal mechanisms by which cellular functions are regulated in eukaryotic cells in response to external stimuli (1). The enzymes catalyzing these phosphorylations, the protein kinases, are tightly regulated and maintained in an inactive state in the absence of the specific activating signal. The mechanism for maintaining the inhibited state of any protein kinase is at least as critical for its function as is catalytic efficiency.

Although the family of protein kinases now includes several hundred members (2), cyclic AMP–dependent protein kinase (cAPK) was among the first to be characterized (3). The demonstration of the activation of cAPK by cAMP introduced the hormone second messenger concept, whereby a hormone binding to the extracellular surface led to the generation of a cytoplasmic second messenger (4). Of the protein kinases, cAPK is also one of the simplest and best understood biochemically (5, 6), largely because the regulatory (R) and catalytic (C) components are coded for by separate genes, and the proteins can be readily separated upon activation. The inactive holoenzyme is an R_2C_2 tetramer. Cyclic AMP binding cooperatively causes the

complex to dissociate, thereby releasing an R_2 (cAMP)$_4$ dimer and two free and active C subunits. Both cytoplasmic and nuclear proteins are substrates for cAPK, and when C is not anchored to R in the R_2C_2 complex, it can enter the nucleus (7).

There are two general classes of R subunits, types I and II, and within each class are at least two distinct gene products (2, 6). All R subunits nevertheless retain a well-defined domain structure. At the amino terminus is a dimerization domain, followed by an autoinhibitor site that resembles either a substrate or an inhibitor. This autoinhibitor segment binds to the active site of the catalytic subunit. The R subunits are thus competitive inhibitors of substrate proteins. The carboxyl terminus is comprised of two tandem homologous cAMP binding domains, A and B. Site A is masked in the holoenzyme so that the cooperative activation is mediated by cAMP binding first to site B (8). This triggers a conformational change that makes site A more accessible. Cyclic AMP binding to site A then mediates dissociation of the complex. The two cAMP binding sites can be readily distinguished by several criteria. Site A has a faster off-rate and has a preference for N6-substituted analogs. Site B, with a slower off-rate, is preferred by C2- and C8-substituted analogs (9). The cAMP binding domains are also homologous to the cAMP binding domain of the catabolite gene activator protein (CAP) in *Escherichia coli* (10).

The domain structure of the R subunits, first characterized by limited proteolysis, was subsequently probed with deletion mutants (5). One of the most stable of these mutants has a deletion of 91 residues at the NH$_2$-terminus (11). Although monomeric, it retains the autoinhibitor site as well as

the two cAMP binding sites. It forms a tight complex rapidly with C, and cAMP mediates activation in a manner similar to the tetrameric holoenzyme. Full understanding of the molecular basis for cAMP binding and for holoenzyme activation requires high resolution structures. Crystal structures of the C subunit have been determined (11a). We describe here the structure of the Δ1–91 deletion mutant of the recombinant bovine RIα subunit (rRIα). Even though the dimerization domain is absent, this structure nevertheless reveals the detailed features of each cAMP binding site and provides a molecular basis for the cooperative binding of cAMP and activation of the holoenzyme.

Structure solution. The Δ1–91 rRIα subunit, (Δ1–91)rRIα, was expressed in *E. coli* as described (11). Unlike the full-length R subunit, this deletion mutant is resistant to proteolysis. A typical yield is 200 mg from 4 liters of culture. To generate a heavy atom substitution site, we replaced the Cys residue with Ser at position 145 by the Kunkel method (12). The expression, biochemical properties, and crystallization of (Δ1–91)-rRIα(S145C) are similar to those of (Δ1–91)rRIα.

Crystals of (Δ1–91)rRIα and (Δ1–91)-rR(S145C) were grown by the vapor diffusion method with the hanging-drop procedure in Linbro plastic tissue culture plates at 22°C (13). The drops contained 5 μl of protein stock (8 mg/ml) and 5 μl of reservoir solution. Hexagonal crystals were produced from a reservoir solution of 1.1 to 1.2 M (NH$_4$)$_2$SO$_4$ (grade III, Sigma), 10 to 12.5 percent glycerol (Sigma) and 10 mM dithiothreitol buffered with 80 to 100 mM sodium acetate, pH 5.5; they grew to their maximum size, 0.15 by 0.15 by 1.5 mm, over 3 weeks. They belonged to space group $P6_122$ ($P6_522$), and the unit cell dimensions were $a = b = 88.9$ Å, $c = 179.9$ Å. There was one molecule per asymmetric unit with a Matthews coefficient, V_m, of 2.9 Å^3 per dalton. The solvent content (14) was approximately 57 percent.

Diffraction data for the native and heavy atom derivative crystals were collected initially with the Xuong-Hamlin multiwire area detector system (15) at the NIH National Research Resource at UCSD. The native crystal diffracted to 2.9 Å resolution. Three heavy atom derivatives, namely, two mercury derivatives and a gold derivative, were prepared, and diffraction data to 3.5 Å were collected. The diffraction data for the native protein and the derivatives were again measured to higher resolutions with an MAR image plate scanner at the Stanford Synchrotron Radiation Laboratory (SSRL). The statistics of data collection and the multiple isomorphic replacement (MIR) phases computed with the program

Y. Su, W. R. G. Dostmann, F. W. Herberg, K. Durick, and S. S. Taylor are in the Department of Chemistry and Biochemistry and N-h. Xuong and K. I. Varughese are in the Department of Biology, University of California, San Diego, La Jolla, CA 92093–0654, USA. L. Ten Eyck is at the San Diego Supercomputer Center, La Jolla, CA 92186, USA.

*Present address: Institut für Pharmakologie und Toxicologie, Technische Universität München, Biedersteiner Straße 29, 80802 München, Germany.
†Present address: Ruhr-Universität Bochum, Medizinische Fakiltät, Institut für Physiologische Chemie I, 44780 Bochum, Germany.
‡To whom correspondence should be addressed.

package PHASES (*16*) are listed in Table 1. Solvent-flattening calculations (*17*) with 2.8 Å MIR phases gave an interpretable map. The space group was assigned as $P6_522$ from the right-handedness of the α helices.

After the map was computed with the solvent-flattened phases, model building was done with the graphics programs TOM (*18*) and O (*19*). The program O was used to construct the backbone and side chains based on the Cα trace that was manually generated with the use of TOM. The map showed well-defined electron density for cAMP bound to both domains A and B (Fig. 1). The initial model included two molecules of cAMP and three segments of peptide chains consisting of 190 residues. The coordinates of this model were improved by X-PLOR (*20*) refinement, which gave an R factor of 34.1 percent for data between 10.0 to 3.0 Å. At this stage, using the program SIGMAA (*21*), we combined phases from the refined partial model with the MIR phases, and the resultant map revealed better electron density for the unbuilt regions. Seventy-four more residues were incorporated into the model after several rounds of model building and phase combinations. The refinement was done iteratively with X-PLOR and omit maps. At present, model consists of 2020 nonhydrogen atoms. The NH_2-terminal residues 92 to 112 and the COOH-terminal residues 377 to 379 could not be traced. Five other regions of the chain consisting of residues 113 to 118, 275 to 279, 285 to 288, 302 to 311, and 375 to 376 showed up in the map with densities less well defined compared to the rest of the structure; however, these residues could be traced and were included in the refinements. These regions were all solvent-exposed. Residues 302 to 311, located in the surface loop connecting β4 and β5 of domain B, have high B factors.

Side chains were assigned as follows. Cys^{145} and Cys^{360} were identified from the positions of the mercury atoms in the derivatives. In each domain, conserved residues interacting with cAMP, Glu^{200}, and Arg^{209} in domain A and Glu^{324} and Arg^{333}

Table 1. Diffraction data and structure solution statistics. N, number of observations, $R_{deriv} = \Sigma|F_p - F_{ph}|/\Sigma F_p$. $R_{sym} = \Sigma_h\Sigma^N_{i=1}|I(h) - I(h)_i|/\Sigma_h\Sigma^N_{i=1}I(h)_i$, where $I(h)_i$ is the ith measurement of reflection h and $I(h)$ is the mean value of the N equivalent reflections. The R derivative is calculated with respect to a merged data set obtained by merging the two data sets. F_H, average root-mean-square (rms) heavy atom structure factor amplitude. F_{anom}, average anomalous dispersion structure factor amplitude of heavy atoms. E, rms closure error. Centric $R, |F_{ph}(obs) - F_{ph}(calc)| \times 100/\Sigma|F_{ph}(obs) - F_p|$; E_{anom}, rms anomalous closure error. The Au derivative was formed by soaking the crystal in solutions of 2 mM $KAuCl_4$. The Hg derivative was obtained by cocrystallizing with C_2H_5HgCl. The protein has two cysteines, one at residue 345 and the other at residue 360; however, only Cys^{360} reacted with Hg. For obtaining another Hg derivative, a new mutant was created by replacing Ser^{145} with Cys. Soaking of crystals of this mutant with 6 mM p-chloromercuribenzene sulfonate (PCMBS) yielded a derivative with two Hg sites. Diffraction data from two native crystals were measured at UCSD (λ=1.518 Å). These two data sets were merged with a native data set measured at SSRL (λ = 1.08 Å) on a MAR image plate; the program MOSFLM (*45*), was used to reduce the data from SSRL. The Hg atom position in the C_2H_5HgCl derivative was located from the isomorphous difference Patterson map. The Au position and the positions of the two Hg atoms in the S145C mutant derivative were located with cross-difference electron density maps. The solvent-flattening calculations were done according to Wang et al. (*17*), on the basis of an assumed solvent content of 50 percent. After convergence, the mean figure of merit was 0.84 with the map inversion R factor of 29 percent. An analysis of the diffraction pattern revealed that the overall temperature factor of the crystal is anisotropic. Hence an anisotropic correction was applied. After the correction, the refinement provided an R factor of 22.1 percent from the previous R of 25 percent. Further refinement with the program TNT (*46*) with all the data yielded the final R of 22.9 percent. As the high resolution data were affected by decay, we confirmed our present refinement to 2.8 Å data.

Data sets used in the structure determination

Data set	Reflections (N)	Observations (N)	d_{min} (Å)	R_{sym} (%)	Overall complete (%)	R_{deriv} (%)	Device
Native 1	8904	61857	3.0	4.8	99.3		Multiwire
Native 2	15809	37561	2.4	5.5	88.5		MAR(SSRL)
C_2H_5HgCl	14656	53743	2.5	7.5	95.0	7.8	MAR(SSRL)
$KAuCl_4$	9494	19257	2.7	6.9	83.8	11.8	MAR(SSRL)
Hg derivative of S145C mutant	9801	52070	2.8	8.9	88.7	10.7	MAR(SSRL)

MIR statistics of the heavy atom derivatives

Derivative	Measurement	Average resolution of the shell (Å)										
		Overall	9.16	5.57	4.63	4.12	3.77	3.51	3.31	3.15	3.01	2.87
C_2H_5HgCl	F_H/E	1.96	1.81	2.29	1.90	1.72	1.92	1.96	2.07	1.97	2.08	2.11
	F_{anom}/E_{anom}	2.02	1.89	2.15	1.76	1.83	2.05	2.03	2.24	2.21	2.40	1.95
	Centric R	0.68										
$KAuCl_4$	F_H/E	1.40	1.58	1.84	1.54	1.36	1.24	1.26	1.44	1.27	1.21	1.29
	Centric R	0.58										
Hg derivative of S145C mutant	F_H/E	2.08	2.32	2.36	1.99	1.88	2.01	2.07	2.15	1.96	2.02	1.98
	Centric R	0.64										
Figure of merit		0.66	0.737	0.714	0.684	0.686	0.674	0.648	0.656	0.622	0.576	0.563

Refinement

Model	Final R factor	B factor	Data selection	Programs
190 residues + 2 cAMP	34.1	Overall	10.0–3.0 Å $I/\sigma>2$	X-PLOR
247 residues + 2 cAMP	25.0	Individual	10.0–2.8 Å $I/\sigma>2$	X-PLOR
264 residues + 2 cAMP	22.1	Individual	8.0–2.8 Å $I/\sigma>2$	X-PLOR
264 residues + 2 cAMP	22.9	Fixed	15.0–2.8 Å all F	TNT

in domain B, were identified. Trp^{260} was identified by its proximity to the adenine ring in domain A. With these residues as markers, side chains were eventually assigned for all the remaining residues. At present, the R factor for the model is 21.7 percent for all the data between 8 to 2.8 Å with $I/\sigma \geq 2.0$ (Table 1). The root-mean-square (rms) deviations from ideal bond length and angles are 0.019 Å and 2.8°, respectively. Ramachandran plots of ϕ, Ψ angles (22) showed that most of nonglycine and nonproline residues are within the allowed regions with 82.3 percent of the 232 residues in the energetically most favored areas. Only eight nonglycine residues fall into the generously allowed regions. Five of these residues, Pro^{117}, Lys^{118}, Arg^{304}, Glu^{306}, and Glu^{308}, are located in regions where electron density is less ordered, as indicated above. The other three residues,

Glu^{187}, Ser^{319}, and Asn^{330}, are in surface loops.

Molecular architecture. The molecule is a monomer with an α/β structure consisting of two cAMP binding domains, each having a similar folding pattern to the cAMP binding domain of CAP (Fig. 2). To simplify comparisons, we have adopted a nomenclature based on CAP, and we aligned the sequences of the cAMP binding domains in CAP, RIα, and RIIα (Fig. 3). The first 21 residues of this deletion mutant are not seen, presumably because this region is disordered. This segment includes the autoinhibitor site that mimics the substrate recognition site and binds to the active site of C. The structure begins with Arg^{113} followed by a helix (α-X:N) (see legend to Fig. 2 for nomenclature). An extended chain then turns into cAMP binding domain A. The COOH-terminus of domain A goes imme-

diately into domain B. The last three residues are disordered and not seen. The molecule is elongated with overall dimensions of 65 Å by 45 Å by 34 Å consistent with earlier estimates of dimensional asymmetry based on the Stokes radius (27.5 Å) (11). The distances between the two cAMP molecules is approximately 26 Å.

The specific topography of each cAMP binding domain (Fig. 4) consists of three major α helices and eight β strands. The eight β strands form a flattened β barrel, consisting of two antiparallel β sheets, each with four strands, connected in a jelly-roll topology. The V-shaped pocket in this jelly-roll β barrel forms a major part of the cAMP binding site. The three helices are connected to the ends of the β barrel. Helix A is at the NH_2-terminus and helix B, followed immediately by helix C, is at the COOH-terminus. Helices A and B are antiparallel. Between strands 6 and 7 is a short helix, α-B', sitting on the top edge of the jelly roll. The phosphate group of the cAMP is located near the NH_2-terminus of this helix and, as discussed later, the capping of this helix is integrally dependent on cAMP.

Cyclic AMP binding sites. In both domains cAMP is bound in a *syn* conformation. The phosphate and the ribose ring interact with the protein through several hydrogen bonds and electrostatic contacts. These interactions mostly occur among highly conserved residues in the segment linking β strands 6 and 7. In contrast, the adenine ring interacts primarily through hydrophobic and stacking interactions with residues in and near the C helix. The nucleotide is thus sandwiched between the β barrel and the C helix. The conserved residues, Glu^{200} and Arg^{209} in domain A and Glu^{324} and Arg^{333} in domain B, participate directly in cAMP binding. The Glu residues interact with the 2'-OH of the ribose ring while the Arg residues interact with the phosphate. In both sites, an aromatic side chain, Trp^{260} in domain A and Tyr^{371} in domain B, stacks with the adenine ring.

While Fig. 4, A and B, shows the general features of each cAMP binding domain, the multiple contacts between cAMP and the protein are summarized in detail in Fig. 4, C and D. The region extending from Gly^{199} to Ala^{210} in site A and from Gly^{323} to Ala^{334} in site B are linked by an extensive network of contacts that are synergistically dependent on the presence of cAMP. For example, Glu^{200} makes multiple contacts. In addition to its interaction with the ribose 2'-OH, it also hydrogen bonds to the Nϵ1 of Trp^{260} and is stabilized by electrostatic contacts with Arg^{241}. Glu^{200} also begins the one-and-a-half-turn helix. Most of the unpaired amides at the beginning of this helix are capped by interactions with protein side
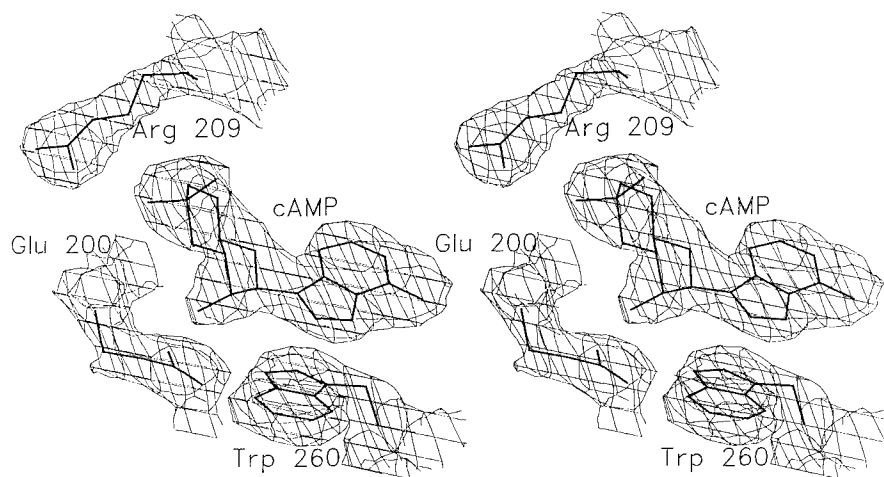

Fig. 1. Stereo view of the ($2F_o - F_c$) electron density of the cAMP binding regions of domain A at 2.8 Å resolution. The map is contoured at 1.5 sigma; cAMP and three residues, Glu^{200}, Arg^{209}, and Trp^{260}, with prominent interactions are shown.
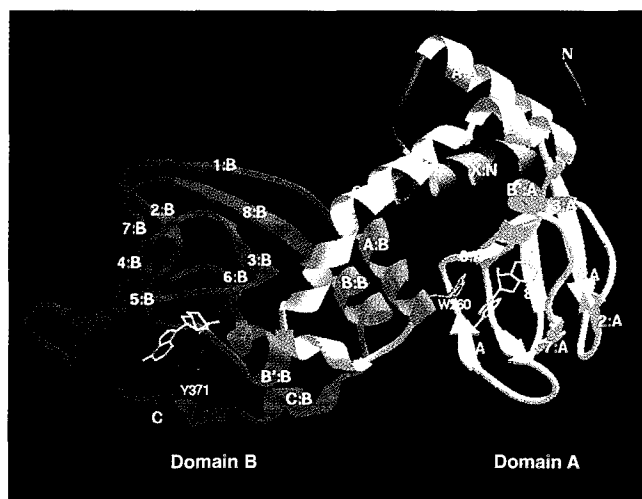
Fig. 2. General architecture of (Δ1–91)rRIα. The three domains, shown as a ribbon representation of the backbone, are colored with the NH_2-terminal region in gray, domain A in cyan, domain B in magenta, and cAMP in yellow. W^{260} and Y^{371}, affinity labeled by 8-N3–cAMP, are shown in red. For nomenclature we have adopted the numbering used for the cAMP binding domain of CAP. The three major helices in domain A are named αA:A, αB:A, and αC:A, and the corresponding helices in domain B are named αA:B, αB:B, αC:B, (Fig. 3). Each β strand is likewise designat-

ed β1:A, β2:A. . .β8:A in domain A and β1:B, β2:B, and so forth in domain B. In that the NH_2-terminus is missing in this deletion mutant, the first helix is designated at present as α-X:N.

chains or by cAMP. For example, the αNH of Glu[199], conserved so far in all of these cAMP binding sites, hydrogen bonds to the 2'-OH of cAMP. The αNH of Glu[200] hydrogen bonds to the Oε2 of its own side chain. The αNH of Ala[202] hydrogen bonds to the equatorial oxygen of the phosphate in cAMP. The αNH of Leu[203] hydrogen bonds to the α carbonyl of Leu[201]. Thus, the architecture of this site, and specifically the secondary structure that includes this short helix, is integrally dependent on the presence of cAMP itself. The stacking of the adenine ring with Trp[260] also depends on this network of interactions involving Glu[200]. The Arg[209] plays a major structural role in addition to binding cAMP. It contributes to cAMP binding by interacting with the equatorial exocyclic oxygen of the cAMP phosphate. This same Nη nitrogen also is only 3.5 Å from the backbone carbonyl of Gly[199]. Thus Arg[209] bridges the conserved segment that links β strands 6 and 7. However, by contacting the backbone carbonyl of Asn[171] in β strand 3 and the side chain carboxylate of Asp[170], it bridges the cAMP binding domain and transmits a signal that extends beyond the immediate cAMP binding site. The interaction with Asp[170] also contributes to the neutralization of the charge on Arg[209].

A similar network of contacts is found in site B (Fig. 4D). Glu[324] hydrogen bonds with the 2'-OH of the ribose ring, to the phenolic OH of Tyr[371], and interacts with its own backbone amide. The aromatic side chain at the end of the C helix is thus positioned both by its stacking with the adenine ring of cAMP and by hydrogen bonding to a conserved residue in the β barrel. Likewise, the backbone amide of Gly[323] also interacts with the 2'-OH of the ribose, and Glu[324] is followed by a short helix. Most of the unpaired αNH groups at the beginning of this helix also hydrogen bond in a manner similar to that in domain A. Unlike Glu[200], Glu[324] does not interact with an Arg comparable to Arg[241]. As in domain A, conserved Arg[333] forms a single ion pair with the equatorial phosphate oxygen of cAMP but also plays a structural role by interacting with the backbone carbonyls of Gly[323] and Glu[289], which is in β strand 3, similar to domain A. In domain B there is no carboxylate near Arg[333] to help neutralize its charge; but there are still potential interactions with residues that extend from Gly[287] to Glu[289].

In addition to the electrostatic interactions, the tight binding of cAMP with K_d's of 10 to 100 nM involves a number of strong hydrophobic interactions. In site A, one side of the adenine base faces a hydrophobic pocket formed by the side chains of Ala[189], Val[184], Val[182], Ala[210], and Ala[211]. On the other side, the five-member ring of

the adenine base stacks with the indole ring of Trp[260] while the six-member ring has van der Waals contacts with Leu[201]. In cAMP binding site B, the adenine ring is sandwiched by hydrophobic interactions between the side chains of Leu[316], Tyr[371], Ser[373], and Ile[325] on one side and Val[300], Val[313], and Ala[335] on the other. The phenol ring of Tyr[371] also stacks with the adenine ring. The stacking of the aromatic rings of Trp[260] and Tyr[371] with the adenine ring of cAMP also orients the dipole moments of the adenine, Tyr, and Trp rings in an antiparallel alignment as predicted (23). Whereas the dipole moments for the adenine and Trp rings are fixed, the dipole moment of Tyr depends on the rotation of the phenolic hydroxyl group. The hydroxyl group of Tyr[371] is fixed by a hydrogen bond to Glu[324] so that the dipole of Tyr[371] cannot rotate.

In prokaryotes the primary receptor for cAMP is CAP where cAMP binding directly mediates gene expression (24). As predicted by sequence alignments (Fig. 3) (10), the general features of the cAMP domains in CAP and R are conserved although we were unable to solve the structure by molecular replacement with the coordinates of CAP. Each cAMP binding domain has three main helices and an eight-stranded β barrel. There are three invariant Gly residues in each domain. One of them (Gly[166] in domain A and Gly[285] in domain B) lies between β2 and β3 and is situated at the third corner of a type II β turn. Type II β turns prefer a Gly residue at this position. The second conserved Gly is located in a loop connecting β3 and β4. The third invariant Gly begins the active site pocket,

Gly[199] in A and Gly[323] in B. A larger side chain here could collide with the adenine ring. Although the fold is conserved, the length of the C helix and its position relative to the β barrel differ in these three structures (Fig. 5). Most significant is the displacement of the C helix in domain A away from the β barrel. As discussed below, two residues, Trp[260] and Arg[241], specifically keep this helix extended away from the barrel.

The different conformation of cAMP, syn in R and anti in CAP, is due most likely to differences in the environment surrounding the adenine rings. The stacking of the adenine ring with aromatic side chains comparable to Trp[260] and Tyr[371], for example, is missing in CAP. Another difference is that the short helix found between β strands 6 and 7 in the R subunits is missing in CAP. CAP has one extra residue in the region that links β6 and β7, and this may prevent the helix from forming. Cyclic AMP binding is three orders of magnitude tighter in R than CAP. The presence of the phosphate:helix interactions and the stacking interactions between the adenine rings and the aromatic side chains probably account for this difference, at least in part.

In eukaryotes, homologous cAMP binding motifs are conserved in the R subunits of cAPK, in the guanosine 3',5'-monophosphate (cGMP)–dependent protein kinase (cGPK), and in the cyclic nucleotide-gated channels (25). The difference in relative specificity for cAMP compared to cGMP is approximately a factor of 100 for cAPK and cGPK (26). One residue that partially accounts for this specificity is the equivalent
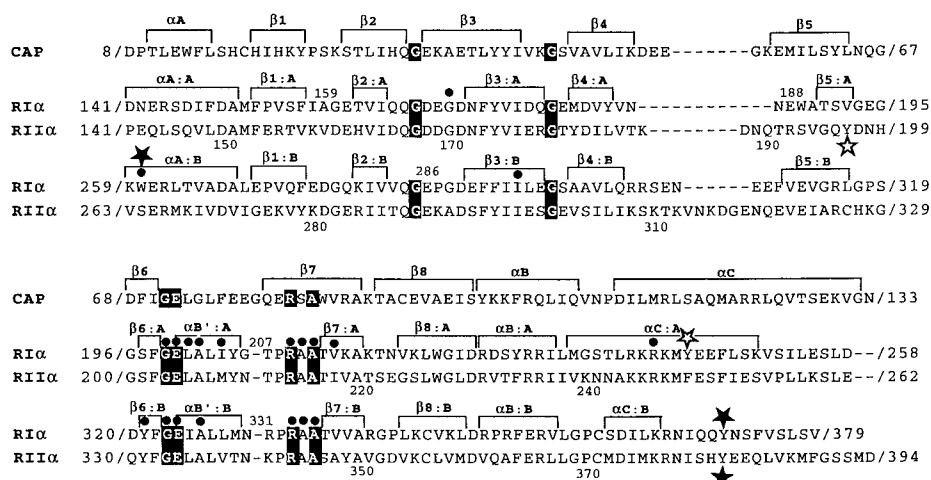

Fig. 3. Sequence alignment of the cAMP binding domains of RI, RII, and CAP. RI corresponds to bovine RIα and RII corresponds to bovine RIIα. Residues that are conserved in all three proteins are indicated by black boxes. Sites of affinity labeling with 8-N3-cAMP in the native protein are indicated by filled stars. Sites affinity labeled in the proteolyzed protein are indicated by open stars. Residues identified as important for cAMP-mediated activation by genetic screening are indicated by black dots. Single-letter abbreviations for the amino acid residues are A, Ala; C, Cys; D, Asp; E, Glu; F, Phe; G, Gly; H, His; I, Ile; K, Lys; L, Leu; M, Met; N, Asn; P, Pro; Q, Gln; R, Arg; S, Ser; T, Thr; V, Val; W, Trp; and Y, Tyr.

of Ala[210] (domain A) and Ala[334] (domain B) in RIα. This is always a Thr in cGPK and an Ala in R. Replacement of these Ala residues with Thr in RIα did improve specificity for cGMP but did not weaken the affinity for cAMP (27). On the basis of the current structure, replacing Ala[210] with Thr and adding an NH$_2$ at the position 6 of cAMP gives a distance of 2.4 Å between the OG1 of Thr and the N2 of cGMP.

Correlation of the structure with chemical data. Affinity labeling with 8-N$_3$-cAMP was used to identify residues near the cAMP binding sites. Two sites were labeled in RIα: Trp[260] in Site A and Tyr[371] in Site B (28). In the RII subunit, Trp[260] is replaced with a Ser and only one site was labeled, Tyr[381], the equivalent of Tyr[371] in RI (29).

Fig. 4. (A and **B**): Overall features of the cAMP binding domains. Ribbon diagrams of domain of cAMP binding domains A and B are shown in (A) and (B), respectively. The general orientation of cAMP (yellow), relative to the β barrel and the C helix is shown. Conserved residues (R[209] and E[200] in domain A and R[333] and E[324] in domain B) are indicated. Stereo views of the hydrogen bonding interactions between cAMP and the protein are shown in (**C**) (site A) and (**D**) (site b). Additional residues, R[241], E[267], and D[170], that interact directly with cAMP domain A are also shown. Possible H bonds are indicated by dashed lines (distances < 3.3 Å). Space-filling models of each cAMP binding site are shown in (**E**) (site A) and (**F**) (site B). Atoms of cAMP and residues involved in cAMP binding are colored differently: carbon in yellow, nitrogen in blue, phosphorus in dark blue, oxygen in red, the others in pink. C8 is the site of attachment of the photoreactive azido moiety.

These two aromatic side chains in RIα are optimally aligned, which presumably accounts for the exceptionally high efficiency in labeling (Fig. 4, E and F).

Affinity labeling of proteolytic fragments and deletion mutants provide an indication of conformational flexibility. For example, when domain B (residues 260 to 379) in RIα is deleted, all the residues normally labeled are absent. In this protein, Tyr[244] was labeled by 8-N$_3$-cAMP (30), indicating that, in the absence of domain B, the C helix in domain A moved closer to the β barrel, thus resembling more closely the orientation in both domain B and CAP (Fig. 5). When the NH$_2$-terminus of the RII subunit was removed by proteolysis (residues 1 to 94), the pattern of photoaffinity labeling also was altered. In this case, Tyr[196] in domain A was labeled, in addition to Tyr[381], indicating that the NH$_2$-terminus also imposed some structural constraints on the COOH-terminal part of the molecule (31).

The chemical features of the two cAMP binding sites were also mapped with cAMP analogs (32). As predicted, no strong hydrogen bonding interactions exist between the adenine ring and the protein; most of the interactions are hydrophobic and stacking. The closest potential hydrogen bond is between the N6 in cAMP bound to domain B and the backbone carbonyl of Asn[372]. Whereas three H bonds between the 2'-, 3'-, and 5'-ribose oxygens were predicted, only the 2'-OH hydrogen bond was observed in the structure. The importance of the exocyclic phosphate oxygens was also correctly predicted. Although the axial oxygen interacts with the amide of Ala[210] and Ala[334], respectively, in site A and B, the equatorial oxygen binds to the side chain of Arg[209] and to the amide of Ala[202] in site A and to Arg[333] and Ala[326] in site B. There is no evidence, however, for a pentacovalent intermediate as was suggested. Analogs also predicted correctly that cAMP binds to R in a *syn* conformation, in contrast to the *anti* conformation seen in CAP.

Analogs also can discriminate between sites A and B (33). Site A can accept analogs having substituents at the C6 position whereas substituents at the C8 position are not well tolerated. The N6 of cAMP bound to site A is exposed, but the accessibility of the C8 position is blocked by the six-member ring of Trp[260], as well as by Val[182] and Val[192]. In contrast, site B prefers analogs substituted at the C8 position, and in this site, the accessibility of the N6 position is blocked by van der Waals contacts with four residues, Tyr[371], Asn[372], Ser[373], and Val[313], the N7-C8 edge of cAMP is accessible (Fig. 4F). Another feature that distinguishes the two sites is the relative off-rates for cAMP. In site B with its slower
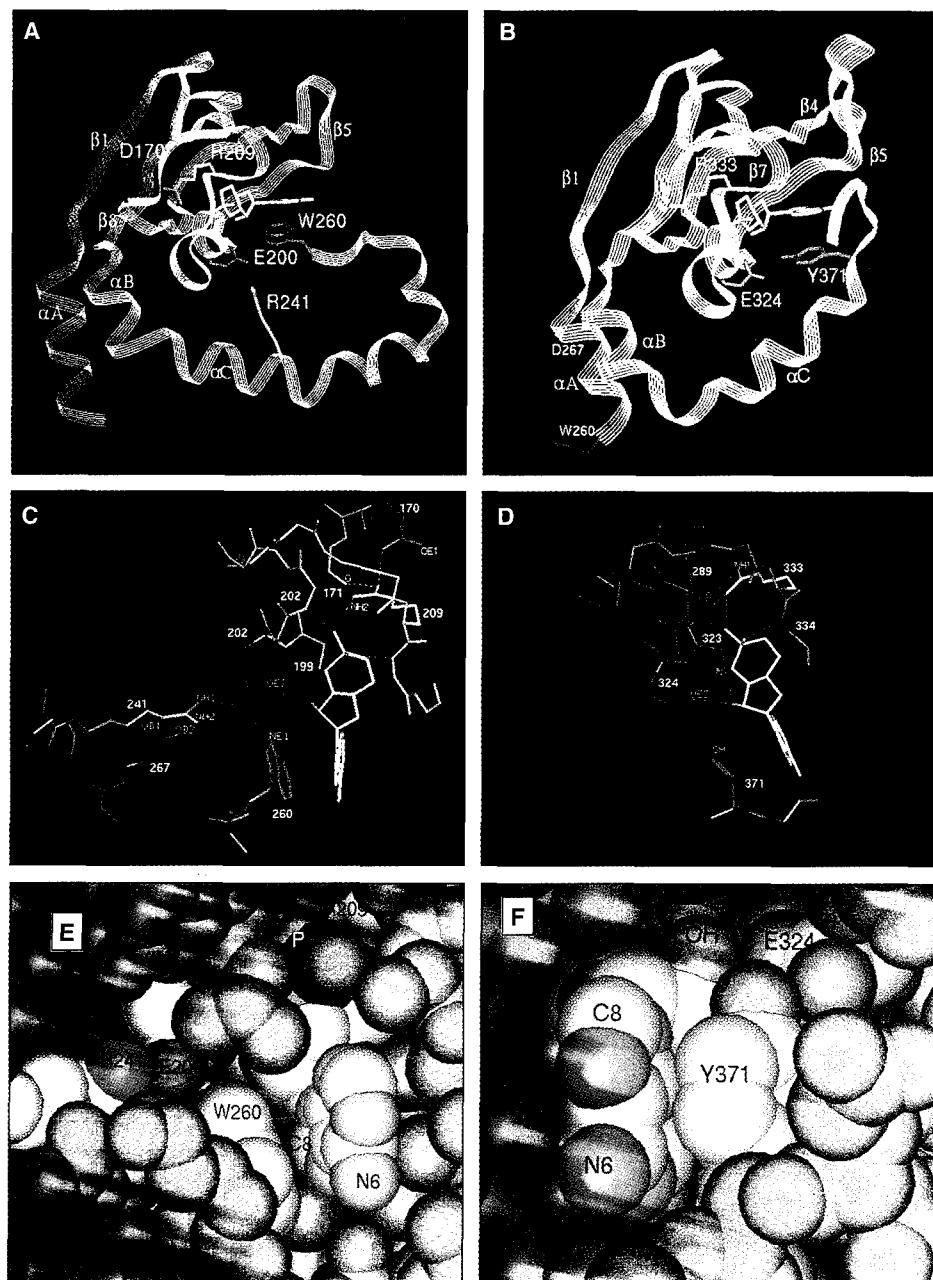
off-rate, the cyclic nucleotide is buried more deeply and is packed tightly against Tyr^{371}. At the base of the cAMP binding pocket, for example, Arg^{333} is completely buried by the nucleotide (Fig. 4F). In contrast, cAMP binds to domain A with a relatively fast off rate. In the crystal structure, this cAMP binding site is more open.

Of the hundreds of cAMP analogs tested, only one group served as antagonists, the chiral phosphorothioate analog (Rp)cAMPS, and its analogs (34). When the sulfur is in the equatorial position, as in (Rp)cAMPS, dissociation of the holoenzyme was blocked, whereas (Sp)cAMPS was an agonist. Sulfur has a larger van der Waals radius (1.70 Å) than oxygen (1.35 Å) (35), and the P-S bond length of the phosphorothioate group is accordingly longer (1.95 Å compared to 1.5 Å). Because most of the charge resides on the sulfur, the resonance of the electrons is also reduced in these chiral analogs (36). Sulfur also does not form hydrogen bonds as well as oxygen. In (Rp)cAMPS, the sulfur replaces the equatorial oxygen that interacts with Arg^{209} and the amide backbone of Ala^{202} in Site A. In the crystal structure the charge of Arg^{209} is neutralized in part by Asp^{170}. With (Rp)-cAMPS bound, the charge of R209 would be neutralized predominantly by the negative charge on the sulfur leaving no anchor for Asp^{170}. The hydrogen bonding to Ala^{202} would also be disturbed. The larger size of the sulfur in both of the chiral analogs probably causes steric hindrance and accounts for their low affinity. At this point, it is not clear why (Sp)cAMPS, and not (Rp)cAMPS, is an antagonist for CAP.

Genetic approaches also identified functionally important residues. The most extensive genetic mapping has been done in RIα of S49 mouse lymphoma cells (37). For these cells cAMP is toxic. By isolating mutants that were resistant to cAMP, a family of RIα mutants defective in cAMP binding were identified. Most of these dominant negative mutations (Fig. 3) are located in the highly conserved β6-β7 loops. Additional residues that lie outside this loop are Gly^{169} and Arg^{241} in domain A and Trp^{260} and Ile^{293} in domain B. Gly^{169} precedes Asp^{170}, which ion pairs with Arg^{209}, and Arg^{241}, which is critical for cooperativity

(38), pairs with Glu^{200}, as predicted (39). In domain B, Trp^{260} stacks with cAMP, and Ile^{293} is at the hydrophobic interface between the two domains. Other mutations, genetically engineered into the RIα subunit, have provided insights into the chemical structure of the cAMP binding sites and the cooperativity between the two sites. Extensive in vitro analysis of mutants such as Arg209Lys, Gly199Glu, and Ala335Asp, has confirmed the importance of these residues for cAMP binding and signaling (40).

Molecular basis for cooperativity. A primary region of contact between domains A and B is an extended hydrophobic surface. Specifically, the hydrophobic surface in domain B formed by Val^{265}, Leu^{269}, Val^{346}, Leu^{294}, Ile^{292}, Tyr^{321}, Leu^{364}, Leu^{357}, Val^{356}, Cys^{360}, and Ile^{363} is covered by Tyr^{244}, Phe^{247}, Leu^{248}, Val^{251}, Ile^{253}, Leu^{254}, and Leu^{257} from domain A (Fig. 6). In addition, the ends of αA:B are anchored by further electrostatic and hydrophobic interactions with domain A. Trp^{260}, which is a critical residue that links the two domains, was first indicated to be important by affinity labeling (28). It lies at the beginning of αA:B and is thus part of the secondary structure of domain B, yet its side chain interacts directly with cAMP binding site A by stacking with the adenine ring and by hydrogen bonding to the conserved Glu^{200} (Fig. 6). Thus it is an integral part of the network of contacts that define cAMP
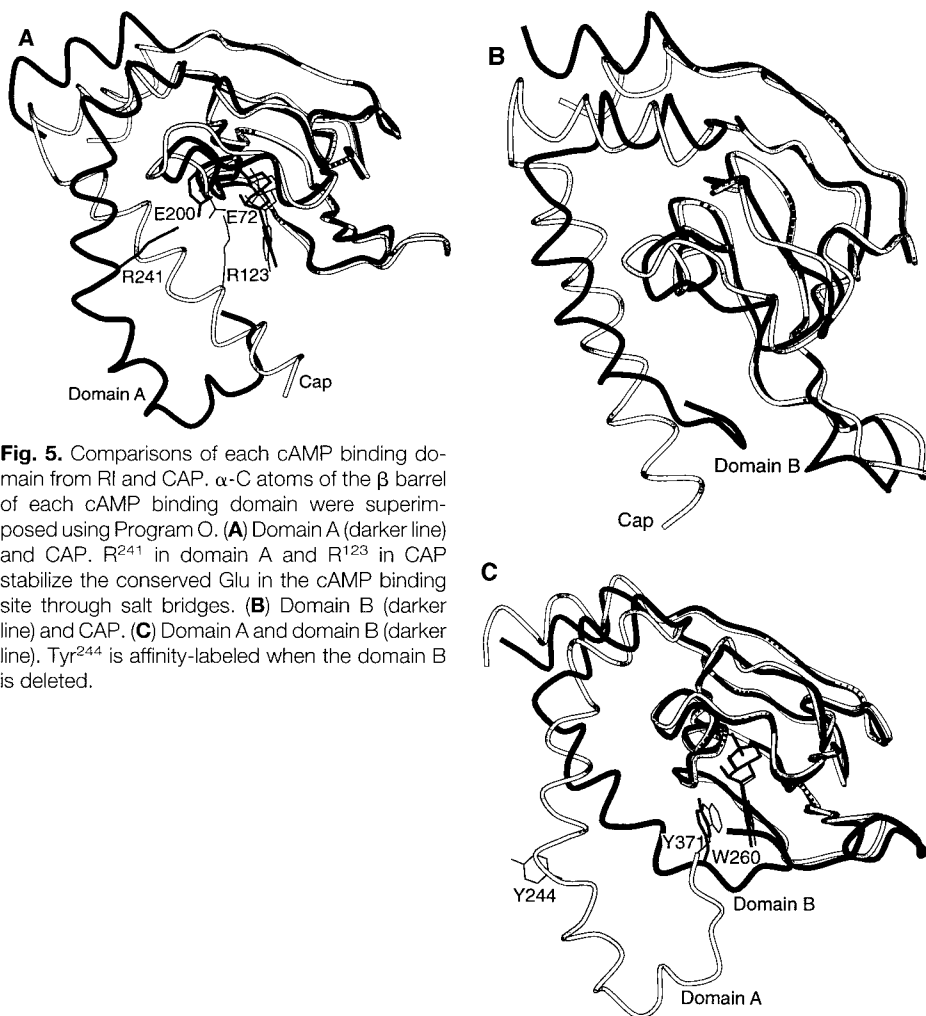

Fig. 5. Comparisons of each cAMP binding domain from RI and CAP. α-C atoms of the β barrel of each cAMP binding domain were superimposed using Program O. (**A**) Domain A (darker line) and CAP. R^{241} in domain A and R^{123} in CAP stabilize the conserved Glu in the cAMP binding site through salt bridges. (**B**) Domain B (darker line) and CAP. (**C**) Domain A and domain B (darker line). Tyr^{244} is affinity-labeled when the domain B is deleted.
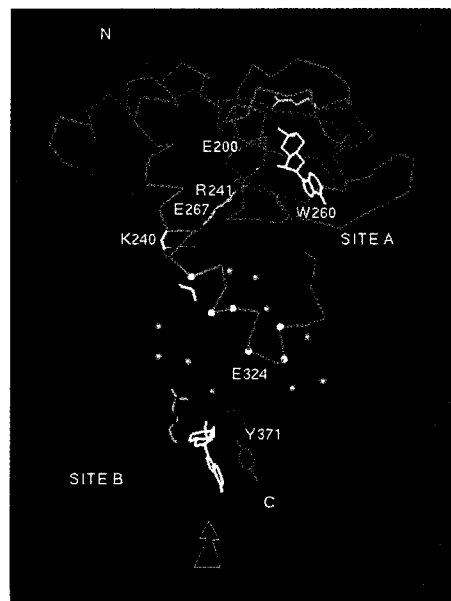

Fig. 6. Interactions between domains A and B. The α carbons of residues that participate in hydrophobic interactions between the two domains are indicated as balls. Additional residues that could play a role in mediating allosteric interactions are indicated (E^{200}, R^{209}, K^{240}, R^{241}, W^{260}, E^{267}, E^{324}, R^{333}, Y^{371}), as are the bound cAMP molecules. The arrow indicates the site where cAMP binds first in the holoenzyme.

binding site A. Another interdomain hydrogen bond interaction involves the side chain of Lys^{240} in αC:A, which hydrogen bonds to the backbone carbonyls of Asp^{267} and Leu^{269} at the COOH-terminus of αA:B. Finally, there is an electrostatic interaction between Arg^{241} and Asp^{267}. Thus the A helix of domain B is anchored firmly to key regions of site A by hydrophobic, electrostatic, and hydrogen bonding interactions.

One question relating to the R subunits of cAPK is how the cooperative binding of cAMP leads to the dissociation, and thus activation, of the holoenzyme. Although we cannot fully understand this process until a structure of the holoenzyme is solved, we can begin to understand how communication between sites A and B and the C subunit might be mediated from the structure of the R subunit. A deletion mutant lacking domain B (Δ260–379) and even a double mutant, where both the NH_2-terminus (Δ1–91) and domain B are deleted, still bind C tightly (11, 41), demonstrating that domain B is not required for high affinity binding to C. On the basis of kinetic arguments, site A is masked in the holoenzyme (8). Thus, in the sequential cooperative pathway for activation of cAPK, cAMP binds first to site B, which "opens up" site A allowing cAMP to bind and C to be released.

There are only two stable conformations of the R subunit; the cAMP-saturated, dissociated R and the holoenzyme. The interactions between domains A and B as well as the immediate environment of each cAMP binding site must be different in these two structures. Since no structure of any cAMP-free domain is yet available, we can only speculate on the conformational changes that take place. The C helices, however, probably play an important role in both domains. The aromatic side chains of Trp^{260} and Tyr^{371}, for example, are packed tightly against the cAMP ligands and have no contacts on the sides away from cAMP. They must therefore either collapse into the cAMP binding pocket in the absence of cAMP or otherwise rearrange. The C helix in domain A also is slightly bent suggesting a strained conformation. When cAMP binds to site B in the holoenzyme and stacks with Tyr^{371}, the orientation of the C helix relative to the β barrel has to change. The fact that cooperativity is lost when Tyr^{371} is replaced with Phe (42) confirms the importance of this initial binding of cAMP to domain B and suggests that the strong dipole-dipole interaction between cAMP and Tyr^{371} is important. The cAMP binding to site B will also influence the position of the NH_2-terminus of αC:B. Two residues here, Cys^{360} and Ile^{363}, are directly involved in the hydrophobic interactions between the two domains. The equivalent of Cys^{360} in

RII is more accessible in the holoenzyme than in the dissociated $R_2(cAMP)_4$ (43) (Fig. 6). As indicated earlier, this hydrophobic region is linked in multiple ways to cAMP binding site A with Asp^{267} and Trp^{260} being of particular importance. Replacement of Arg^{241}, which binds directly to both Asp^{267} in domain B and Glu^{200} in domain A, with Ser or Lys demonstrated that this residue is a key feature for the allosteric coupling between sites A and B (38). Thus communication between the two domains is likely carried out through the C helix of domain B to the interdomain hydrophobic interaction region and transmitted to site A through residues Asp^{267}, Arg^{241}, Glu^{200}, and Trp^{260} or vice versa.

When holoenzyme forms, the initial docking of C to R involves interactions of the autoinhibitor site in R with the active site cleft in C. This autoinhibitor site in the free R subunit is extremely labile to proteolysis (5, 6) and, in our structure, the first 21 residues are disordered. This initial interaction is essential; however, it is not sufficient to convey high affinity binding. To achieve high affinity binding requires interactions involving the surface of C that lies COOH-terminal to the consensus site peptide. This is the surface that surrounds and includes the essential phosphorylation site, Thr^{197} (44). Point mutation of the P-Thr itself as well as the basic residues that bind the phosphate all interfere with R subunit binding. The second step in forming holoenzyme would thus be the docking of the C subunit, with its active site cleft occupied, to a region on cAMP binding domain A. With this structure we can now begin to model these interaction sites.

REFERENCES AND NOTES

1. E. G. Krebs, *Bioscience Rep.* **13**, 127 (1993).
2. S. K. Hanks, *Curr. Biol.* **1**, 369 (1991).
3. D. A. Walsh, J. P. Perkins, E. G. Krebs, *J. Biol. Chem.* **243**, 3763 (1968).
4. E. W. Sutherland and T. W. Rall, *ibid.* **232**, 1077 (1958).
5. S. S. Taylor, J. A. Buechler, W. Yonemoto, *Annu. Rev. Biochem.* **59**, 971 (1990).
6. J. D. Scott, *Pharmacol. Ther.* **55**, 123 (1991).
7. E. A. Nigg, *Adv. Cancer Res.* **55**, 271 (1990). D. A. Fantozzi et al., *J. Biol. Chem.* **269**, 2676 (1994).
8. D. Øgreid and S. O. Døskeland, *FEBS. Lett.* **129**, 287 (1981).
9. D. Øgreid, R. Ekanger, R. H. Suva, J. P. Miller, S. O. Doskeland, *Eur. J. Biochem.* **181**, 19 (1989).
10. I. T. Weber, T. A. Steitz, J. Bubis, S. S. Taylor, *Biochemistry.* **26**, 343 (1987).
11. L. Saraswat, G. E. Ringheim, J. Bubis, S. S. Taylor, *J. Biol. Chem.* **263**, 18241 (1988). F. W. Herberg, W. R. Dostmann, M. Zorn, S. J. Davis, S. S. Taylor, *Biochemistry* **33**, 7485 (1994).
11a. D. R. Knighton et al., *Science* **253**, 407 (1991); *ibid.*, p. 414.
12. T. A. Kunkel, K. Benebek, J. McClary, *Methods Enzymol.* **204**, 125 (1991).
13. Y. Su, S. S. Taylor, W. R. Dostman, N.-h. Xuong, K. I. Varughese, *J. Mol. Biol.* **230**, 1091 (1993).
14. B. W. Matthews, *ibid.* **33**, 491 (1968).
15. N.-h. Xuong, C. Nielson, R. Hamlin, D. Anderson, *J. Appl. Crystallogr.* **18**, 342 (1985).
16. W. Furey and S. Swaminathan, *Am. Crystallogr. Assoc. Mtg. Abstr. Ser. 2.* **18**, 73 (1990).
17. B.-C. Wang, *Methods Enzymol.* **115**, 90 (1985).
18. C. Cambillau and E. Horjales, *J. Mol. Graphics* **5**, 174 (1987).
19. T. A. Jones, J. Y. Zou, S. W. Cowan, M. Kjeldgaard, *Acta Crystallogr.* **47**, 110 (1901).
20. A. T. Brünger, *XPLOR Version 3.1 Manual* (Yale University, New Haven, CT, 1993).
21. R. Read, *Acta Crystallogr.* **A42**, 140 (1986).
22. R. A. Laskowski, M. W. Macarthur, D. S. Moss, J. M. Thornton, *J. Appl. Crystallogr.* **26**, 283 (1993).
23. K. Baldridge and W. R. G. Dostmann, unpublished data.
24. A. Kolb, S. Busby, H. Buc, S. Garges, S. Adhya, *Annu. Rev. Biochem.* **62**, 749 (1993).
25. J. B. Shabb and J. D. Corbin, *J. Biol. Chem.* **267**, 5723 (1992).
26. T. Lincoln and J. D. Corbin, *Adv. Cyclic Nucleic Res.* **15**, 139 (1983).
27. J. B. Shabb, B. D. Buzzeo, L. Ng, J. D. Corbin, *J. Biol. Chem.* **266**, 24320 (1991).
28. J. Bubis and S. S. Taylor, *Biochemistry.* **24**, 2163 (1985); *ibid.* **26**, 3478 (1987).
29. A. R. Kerlavage and S. S. Taylor, *J. Biol. Chem.* **255**, 8483 (1980).
30. G. E. Ringheim, L. D. Saraswat, L. D. Bubis, S. S. Taylor, *ibid.* **263**, 18247 (1988).
31. J. Bubis and S. S. Taylor, *Biochemistry.* **26**, 5997 (1987).
32. R. J. W. DeWit et al., *Eur. J. Biochem.* **152**, 255 (1984); T. S. Yagura and J. P. Miller, *Biochemistry* **20**, 879 (1981); B. Jastorff, J. Hoppe, M. Morr, *Eur. J. Biochem.* **101**, 555 (1979).
33. J. D. Corbin et al., *Eur. J. Biochem.* **125**, 259 (1982); D. Øgreid et al., *ibid.* **150**, 219 (1985); S. R. Rannels and J. D. Corbin, *J. Biol. Chem.* **255**, 7085 (1980).
34. P. J. M. Van Haastert et al., *ibid.* **259**, 10020 (1984); W. Dostmann et al., *ibid.* **265**, 10484 (1990).
35. T. E. Creighton, *Proteins* (Freeman, New York, 1984), p. 139.
36. P. A. Frey and R. D. Sammons, *Science* **228**, 541 (1985).
37. G. S. McKnight et al., *Rec. Prog. Hormone Res.* **44**, 307 (1988). K. A. Gorman and R. A. Steinberg, *Somat. Cell Mol. Genet.* **20**, 301 (1994).
38. M. M. Symcox, R. D. Cauthron, D. Ogreid, R. A. Steinberg, *J. Biol. Chem.* **269**, 23025 (1994).
39. R. A. Steinberg, K. B. Gorman, D. Ogreid, S. O. Doskeland, I. T. Weber, *ibid.* **266**, 3547 (1991); T. A. Woodford, L. A. Correll, G. S. McKnight, *ibid.* **262**, 13321 (1987); E. Duprez et al., *ibid.* **268**, 8832 (1993).
40. J. J. Neitzel, W. R. G. Dostmann, S. S. Taylor, *Biochemistry* **30**, 733 (1991).
41. G. E. Ringheim and S. S. Taylor, *J. Biol. Chem.* **265**, 4800 (1990).
42. J. Bubis, L. D. Saraswat, S. S. Taylor, *Biochemistry* **27**, 1570 (1988).
43. N. Nelson and S. S. Taylor, *J. Biol. Chem.* **258**, 10981 (1983).
44. C. S. Gibbs, D. R. Knighton, J. M. Sowadski, S. S. Taylor. M. J. Zoller, *ibid.* **267**, 4806 (1992); S. A. Orellana, P. S. Amieux, X. Zhao, G. S. McKnight, *ibid.* **268**, 6843 (1993).
45. A. G. W. Leslie in joint CCCP4 and ESF-EACMB Newsletter on Protein Crystallography No. 26 (Daresbury Laboratory, Warrington, UK, 1992).
46. D. E. Tronrud, L. F. Ten Eyck, B. W. Matthews, *Acta Crystallogr.* **A43**, 489 (1987).
47. Supported in part by NIH grants GM34921 (S.S.T.) and RR01644 (N-h.X.), the Lucille P. Markey Charitable Trust (S.S.T., L.T.E., N-h.X.), NSF grant BIR-9223760 (L.T.E.), and Public Health Service Training Grant GM07313 (Y.S.). We thank the San Diego Supercomputer Center for use of the Advanced Scientific Visualization Laboratory and the Cray C90, the Stanford Synchrotron Radiation Laboratory for providing us beam time for data collection, and Xiaoping Dai for his help in data collection and data processing. Coordinates have been deposited on the Brookhaven Protein Data base, with tracking number IRGS.

Communication

Tyrosines outside the Kinase Core and Dimerization Are Required for the Mitogenic Activity of RET/ptc2*

Kyle Durick‡§, Virginia J. Yao‡,
Maria Grazia Borrello¶, Italia Bongarzone¶,
Marco A. Pierotti¶, and Susan S. Taylor‡∥

*From the ‡Department of Chemistry and
Biochemistry, University of California,
San Diego, La Jolla, California 92093-0654
and ¶Divisione di Oncologia Sperimentale A,
Istituto Nazionale Tumori, Milan, Italy*

Defects in the c-*ret* proto-oncogene, a member of the protein tyrosine kinase receptor family, have recently been linked to two types of genetic syndromes, Hirschsprung's disease and the multiple endocrine neoplasia family of inherited cancers. RET/ptc2 is the product of a papillary thyroid carcinoma translocation event between the genes coding for c-*ret* and the type Iα regulatory subunit of protein kinase A (RIα) (Lanzi, C., Borrello, M., Bongarzone, I., Migliazza, A., Fusco, A., Grieco, M., Santoro, M., Gambetta, R., Zunino, F., Della Porta, G., and Pierotti, M. (1992) *Oncogene* 7, 2189–2194). The resulting 596-residue protein contains the first two-thirds of RIα and the entire tyrosine kinase domain of c-*ret* (RET$_{tk}$). An *in vivo* assay of growth stimulatory effects was developed, which consisted of microinjecting a RET/ptc2 expression plasmid into the nuclei of 10T1/2 mouse fibroblasts and observing the incorporation of 5-bromodeoxyuridine. This assay was used to determine that only the dimerization domain of RIα fused to RET$_{tk}$ is required for RET/ptc2's mitogenic activity. In addition, all of the reported Hirschsprung's disease point mutations in the RET$_{tk}$ (S289P, R421Q, and R496G) inactivate RET/ptc2 in our assay, confirming that these are loss of function mutations. Two tyrosines outside the conserved kinase core were also identified that are essential for full mitogenic activity of RET/ptc2. These two tyrosines, Tyr-350 and Tyr-586, are potential sites for Src homology 2 and phosphotyrosine binding domain interactions.

The *ret* oncogene was discovered in transfection experiments where DNA from human lymphomas was introduced into NIH3T3 cells (1). This oncogene was not expressed in the original lymphoma, but instead had arisen from a rearrangement during the transfection, hence the name *ret*. The c-*ret*

proto-oncogene encodes a novel receptor tyrosine kinase with a cadherin-like motif in its extracellular domain (2).

The c-*ret* proto-oncogene is responsible for four human disease syndromes: Hirschsprung's disease, a developmental disorder, and the dominantly inherited cancer syndromes FMTC,[1] MEN2A, and MEN2B. Hirschsprung's disease occurs at a rate of approximately 1 in 6000 live births and is characterized by a lack of parasympathetic innervation of the lower intestine. Occurrence of this disease corresponds to c-*ret* gene deletions and nonsense point mutations leading to truncation of the expressed protein (3, 4). Also, three mutations resulting in single amino acid substitutions in the kinase region of the c-*ret* gene have been reported in Hirschsprung's patients (3, 4). In addition to medullary thyroid carcenoma, the unique pathologic feature of FMTC, MEN2A, and MEN2B patients display additional hyperplasias. These syndromes have been linked to point mutations in the c-*ret* gene (5, 6, 7). Recent evidence suggests that, in the case of the MEN2A, these mutations result in the expression of constitutively activated forms of c-*ret* (8).

It has also been demonstrated that constitutively active forms of the c-*ret* proto-oncogene are present in nearly half of papillary type thyroid carcinomas (9). These oncogenic forms of *ret* are the result of somatic chromosome translocations or inversions, which fused the c-*ret* tyrosine kinase domain (RET$_{tk}$) with different genes. One of the resultant transforming sequences, RET/ptc2 (papillary thyroid carcinoma), was the product of a crossover between the genes coding for c-*ret* and the type Iα regulatory subunit of cyclic-AMP-dependent protein kinase (RIα) (10). The chimeric gene encodes a protein of 596 residues, which contains the first two-thirds of RIα and the entire tyrosine kinase domain of c-*ret* (11). RET/ptc2 is transforming, presumably due to constitutive tyrosine kinase activity, but the structural basis for RET$_{tk}$ activation via fusion to RIα remains unclear.

Here we report the development and use of a microinjection assay to study the mitogenic activity RET/ptc2. Deletion mutants were tested in the assay to determine which portions of RIα were required to elicit the mitogenic activity of RET/ptc2. Only the amino-terminal region of RIα, which encodes a dimerization domain (12), fused to the RET$_{tk}$ was necessary. This portion of RIα was also capable of activating the tyrosine kinase domain of the epidermal growth factor receptor in this assay system. In addition, all of the reported Hirschsprung's disease point mutations in the RET$_{tk}$ inactivated RET/ptc2 in our assay. To begin the search for interaction sites with other signaling proteins, the mitogenic activity of RET/ptc2 mutants lacking single tyrosines was tested. Two tyrosines were found to be essential for the mitogenic activity of RET/ptc2.

EXPERIMENTAL PROCEDURES

Construction of Mammalian Expression Plasmids—The cDNA coding for wild-type RET/ptc2 was excised from a pMAM-neo expression vector previously described (11) using the restriction enzyme *Xba*I. This

[1] The abbreviations used are: FMTC, familial medullary thyroid carcinoma; MEN, multiple endocrine neoplasia; RIα, type Iα regulatory subunit of cAMP-dependent protein kinase (protein kinase A); RET$_{tk}$, tyrosine kinase domain of the c-Ret receptor; SH2, Src homology 2 domain; DMEM, Dulbecco's modified Eagle's medium; FBS, fetal bovine serum; FITC, fluorescein isothiocyanate; BrdUrd, bromodeoxyuridine; EGF, epidermal growth factor.

1

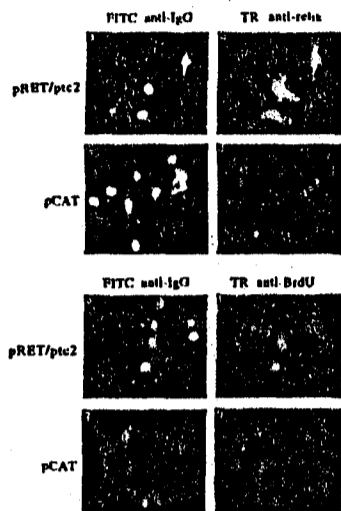2   *RET/ptc2 Mitogenic Activity*

FIG. 1. **Immunostaining for RET/ptc2 expression and 5-bromodeoxyuridine (BrdUrd) incorporation in 10T1/2 cells injected with pRET/ptc2** (*a* and *b*, *e* and *f*) **or pCAT** (*c* and *d*, *g* and *h*) **expression vectors.** *a*, IgG injection marker stained with FITC anti-Guinea pig IgG. *b*, same field of cells as *a*, but showing Texas Red anti-RET_{tk} staining. *c*, IgG injection marker stained with FITC anti-guinea pig IgG. *d*, Same field of cells as *c*, but showing Texas Red anti-RET_{tk} staining. *e*, IgG injection marker stained with FITC anti-rabbit IgG. *f*, Same field of cells as *e*, but showing Texas Red anti-BrdUrd staining. *g*, IgG injection marker stained with FITC anti-rabbit IgG. *h*, Same field of cells as *g*, but showing Texas Red anti-BrdUrd staining.

fragment was then subcloned into the *Xba*I restriction site of the pRc/CMV mammalian expression vector (Invitrogen). Restriction digests were performed to screen for orientation, and then the entire cDNA sequence was verified using dideoxy sequencing (13) with Sequenase version 2.0 (U. S. Biochemical Corp.).

Site-directed mutagenesis was performed with the Kunkle method (14) using the Mutagene kit (Bio-Rad). Constructs expressing deletion mutants of RET/ptc2 were made by introducing *Nhe*I restriction sites flanking the segment of DNA to be deleted, digesting with *Nhe*I, and then ligating the new ends back together. All mutant constructs were sequenced to verify mutagenesis. Supercoiled plasmid DNA expressing various constructs were prepared by double banding in cesium chloride gradients (15).

Cell Culture and Microinjection—Mouse 10T1/2 fibroblasts were plated in Dulbecco's modified Eagle's medium containing 10% fetal bovine serum (DMEM + 10% FBS). The cells were maintained at 37 °C in a 10% CO_2 atmosphere and split just before reaching confluence.

For microinjection, cells were plated on glass coverslips and grown to 70% confluence in DMEM + 10% FBS. The coverslips were then transferred to DMEM containing 0.05% calf serum. After 24 h of incubation in the FBS-free medium, the cells were injected into their nuclei with solutions of injection buffer (20 mM Tris, pH 7.2, 2 mM $MgCl_2$, 0.1 mM EDTA, 20 mM NaCl) containing 100 μg/ml expression plasmid DNA and 6 mg/ml either guinea pig or rabbit IgG (Sigma). All microinjection experiments were performed using an automatic micromanipulator (Eppendorf, Fremont, CA), with glass needles pulled on a vertical pipette puller (Kopf, Tujunga, CA).

Immunostaining—For detection of RET/ptc2 protein, cells were fixed in 3.7% formaldehyde 5 h after injection for 5 min, and then washed with phosphate-buffered saline. The cells were then incubated successively with rabbit anti-RET_{tk} (dilution 1:500), biotinylated donkey anti-rabbit IgG (dilution 1:400, Jackson ImmunoResearch, West Grove, PA), Texas Red streptavidin (dilution 1:100, Amersham Corp.), and FITC anti-guinea pig IgG (dilution 1:100, Jackson). The anti-RET_{tk} antibody is a rabbit polyclonal antibody raised against a synthetic peptide corresponding to residues 535–551 of RET/ptc2 conjugated to keyhole limpet hemocyanin (Calbiochem).

DNA synthesis was assessed through incorporation of the thymidine analog 5-bromodeoxyuridine (BrdUrd) and its subsequent detection by immunostaining (16). Following nuclear microinjection, 0.1% BrdUrd labeling reagent (Amersham) was added to the starvation medium (DMEM + 0.05% calf serum), and the cells were incubated for an additional 24 h. Cells were fixed in 95% ethanol, 5% acetic acid for 30
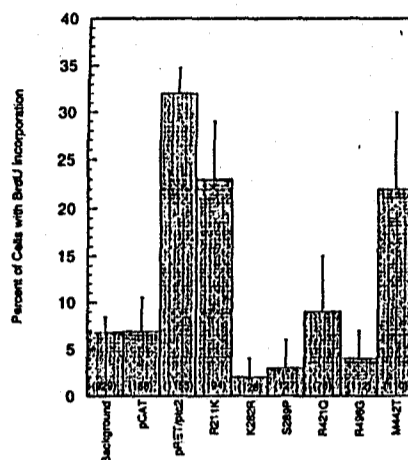

FIG. 2. **Mitogenic activity of RET/ptc2 point mutants.** The fraction of injected cells that stained positive for BrdUrd incorporation is shown for various plasmids expressing either wild-type RET/ptc2 or RET/ptc2 point mutants. In each case the plasmids were injected at a concentration of 100 μg/ml. The column labeled background represents uninjected cells under the assay conditions. The error bars show the 95% confidence interval calculated using the standard error of proportion. The *number* in *parentheses* is the total number of injected cells.

min, and then washed with phosphate-buffered saline. Incorporation of 5-bromodeoxyuridine was visualized by successively incubating the fixed cells with mouse anti-bromodeoxyuridine (undiluted, Amersham), biotinylated donkey anti-mouse IgG (dilution 1:500, Jackson), Texas Red streptavidin (dilution 1:100, Amersham), and FITC anti-rabbit IgG (dilution 1:100, Jackson).

RESULTS AND DISCUSSION

Development of Mitogenic Assay—To evaluate which structural features of RET/ptc2 are essential for its mitogenic activity, an expression plasmid microinjection assay was developed. This assay allows for both rapid screening of protein expression and evaluation of mitogenic activity. The expression vector, pRET/ptc2, was co-injected into nuclei of serum-starved 10T1/2 fibroblasts with rabbit or guinea pig IgG, which served as an injection marker. After incubation for 24 h in 5-bromodeoxyuridine (BrdUrd)-containing starvation medium, the cells were fixed and stained for the IgG-injection marker and either for RET_{tk} protein expression (Fig. 1, *b* and *d*) or DNA synthesis as assessed by BrdUrd incorporation (Fig. 1, *f* and *h*). An identical construct containing the chloramphenicol acetyltransferase gene (pCAT) was used as a negative control.

Cells injected with pRET/ptc2 expressed protein detectable by anti-RET_{tk} antibodies as early as 5 h post-injection (Fig. 1*b*). The expressed protein was cytoplasmic, and the amount and distribution of expressed protein was indistinguishable from that observed in pRET/ptc2-injected cells for all of the mutants discussed in this paper (data not shown). A plasmid concentration of 100 μg/ml was chosen for injections. Under these conditions, over 30% of the pRET/ptc2-injected cells entered S phase, compared to less than 6% of the pCAT-injected cells (Fig. 2).

Consequences of Mutations in ret—Using this assay, the mitogenic activity of various RET/ptc2 point mutants was tested (Fig. 2). To determine whether cAMP binding was important for RET/ptc2 activity, Arg-211 was mutated to Lys. This change eliminates high affinity cAMP binding in the A binding site of RIα (17); however, this point mutation had no significant effect on RET/ptc2 mitogenic activity. In contrast, elimination of a conserved Lys in the kinase domain (18), K282R, eliminated *in vivo* mitogenic activity. Likewise, the three reported Hirschsprung's disease point mutations located in the c-Ret tyrosine kinase domain, S289P, R421Q, and R496G, all inacti-

Orig. Op.	OPERATOR:	PROOF:	PE's:	AA's:	COMMENTS:		ARTNO:
1st K35, 2nd	judy						352754

a

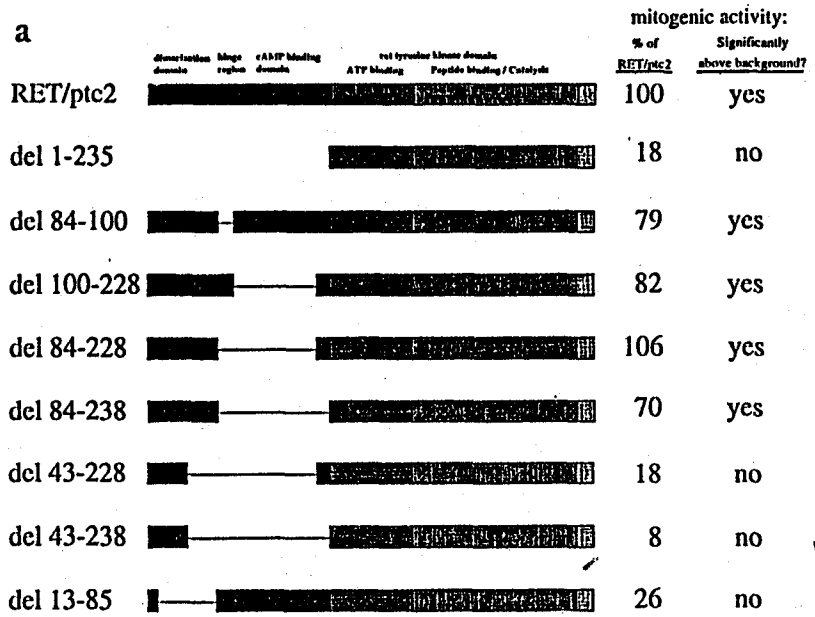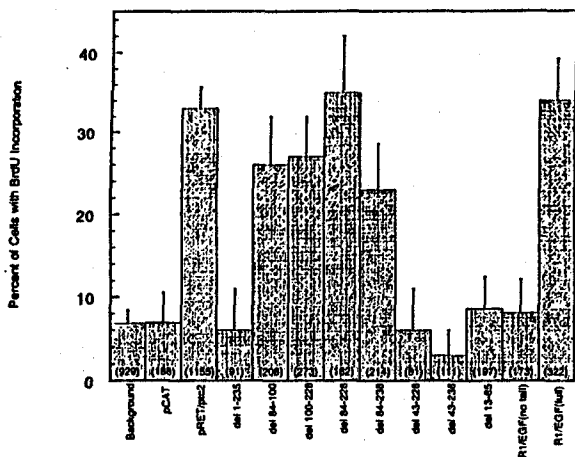|	mitogenic activity: % of RET/ptc2	Significantly above background?
RET/ptc2	100	yes
del 1-235	18	no
del 84-100	79	yes
del 100-228	82	yes
del 84-228	106	yes
del 84-238	70	yes
del 43-228	18	no
del 43-238	8	no
del 13-85	26	no

b

FIG. 3. **Mitogenic activity of RET/ptc2 deletion mutants.** *a*, schematic representation of the deletion mutants tested. In the RIα subunit the dimerization domain includes residues 1–84, the hinge region consists of residues 86–99, and the cAMP binding domain extends from residues 100 through 236. *b*, the fraction of injected cells that stained positive for BrdUrd incorporation is shown for various plasmids expressing either wild-type RET/ptc2, RET/ptc2 deletion mutants, RIα/EGF receptor kinase chimera, or RIα/EGF receptor kinase without its carboxyl-terminal tail (see text). Plasmids were injected at a concentration of 100 μg/ml. The error bars show the 95% confidence interval calculated using the standard error of proportion. The number in parentheses is the total number of injected cells.

vated RET/ptc2 in this assay. These results support the model that Hirschsprung's disease results from a loss of c-Ret function and are consistent with recently obtained results using transfection assays on NIH3T3 and PC12 cell lines (19). The MEN2B mutation (M442T) had no effect on this activated form of c-Ret, which does not contradict a recent report that this mutation alters substrate specificity rather than catalytic activity of c-*ret* (8).

Role of RIα in RET/ptc2—The NH$_2$ terminus of RET/ptc2 comprises the first 236 residues of RIα, which includes the RIα dimerization domain, the cAMP-dependent protein kinase autoinhibitory site, and most of RIα's first cAMP binding domain (20). This is fused to the cytoplasmic portion of the RET receptor, which consists of its tyrosine kinase domain (RET$_{tk}$) followed by a short COOH-terminal tail. The wild-type RIα subunit is a disulfide-bonded dimer with the protomers aligned through residue 37 in an antiparallel orientation (12). Constructs expressing deletion mutants were tested to determine the role of RIα in the activation of RET$_{tk}$ (Fig. 3). These mutants showed clearly that the only portion of RIα required for RET/ptc2 mitogenic activity was the dimerization domain (Fig. 3*b*) and support the hypothesis that the RET$_{tk}$ is activated in RET/ptc2 via the dimerization domain of RIα. One model for

receptor tyrosine kinase activation is through ligand-induced dimerization, or oligomerization, followed by trans-phosphorylation (21, 22). This would occur through a parallel orientation of dimerized receptors, since both monomers are membrane-bound. In contrast, the dimerization domain of RIα may provide an antiparallel orientation (12) for the linked monomers, and we are currently investigating the structural basis for this novel receptor tyrosine kinase activation mechanism *in vitro*.

To investigate whether RIα-mediated dimerization is a general activating motif for receptor tyrosine kinases, an analogous construct to RET/ptc2 was made by substituting the epidermal growth factor receptor tyrosine kinase (EGF$_{tk}$) for the RET$_{tk}$. The expression construct encoding RIα residues 1–236 fused to the EGF$_{tk}$ and its COOH-terminal tail, residues 647-1186, was as active as pRET/ptc2 in our microinjection assay (Fig. 3*b*). The carboxyl-terminal tail, residues 959-1186, contains all of the known Src homology 2 domain (SH2) docking sites of the EGF receptor (23). Deletion of this tail in the RIα/EGF$_{tk}$ construct eliminated its mitogenic response in our assay (Fig. 3*b*). COOH-terminal truncations of the holo-EGF receptor have been shown to have increased transforming activity, attributed to an inability to internalize and attenuate the EGF signal (24, 25). The complete loss of mitogenic activity

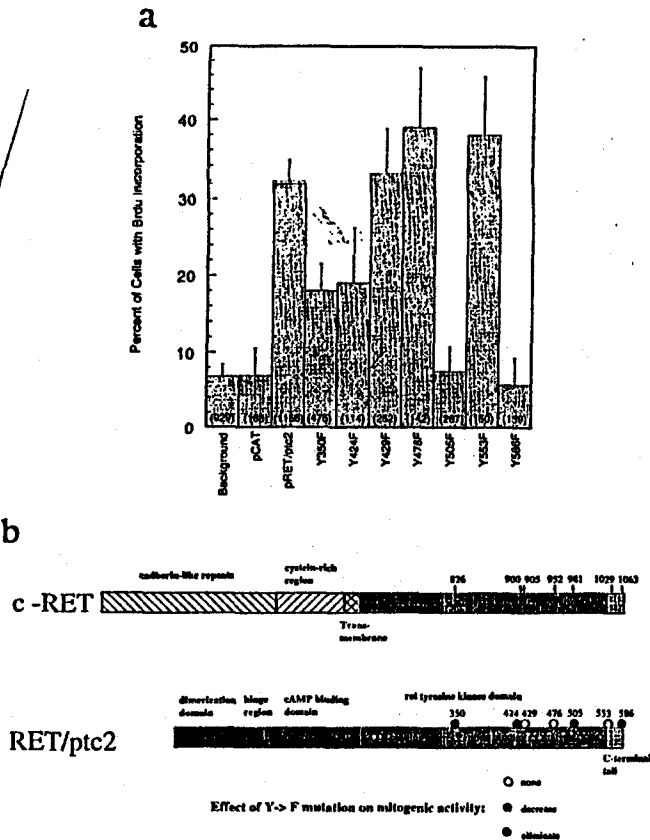4(8)   *RET/ptc2 Mitogenic Activity*

a

b

FIG. 4. **Mitogenic activity of RET/ptc2 tyrosine to phenylala-
nine mutants.** *a*, the fraction of injected cells which stained positive for
BrdUrd incorporation is shown for various plasmids expressing either
wild-type RET/ptc2 or RET/ptc2 Tyr to Phe point mutants. Plasmids
were injected at a concentration of 100 μg/ml. The *column* labeled
background represents uninjected cells under the assay conditions. The
error bars show the 95% confidence interval calculated using the stand-
ard error of proportion. The *number* in *parentheses* is the total number
of injected cells. *b*, schematic representation of RET/ptc2 showing the
locations of the seven tyrosines mutated to phenylalanine. The kinase
domain of RET extends from residues 237 to 545 of RET/ptc2, the
COOH-terminal tail ends at residue 596, and the platelet-derived
growth factor-like insert of RET encompasses residues 344–367. The
corresponding tyrosines are shown on the c-Ret schematic (2).

for our COOH-terminal EGF$_{tk}$ deletion suggests that SH2 do-
main interactions are more important for the mitogenic re-
sponse of RIα/EGF$_{tk}$ than for COOH-terminal truncations of
the holo-EGF receptor.

Role of Tyrosines in RET/ptc2—To identify possible SH2
interaction sites in RET/ptc2, several tyrosines were mutated
to Phe and the resultant mutants tested for mitogenic activity
(Fig. 4). Of the seven Tyr mutants, two, Y350F and Y424F,
exhibited significantly reduced mitogenic activity. Mutations
at two other tyrosines, Y505F and Y586F, abolished the mito-
genic effect. Tyr-350 is located in a variable insert region of
receptor tyrosine kinases, and in the platelet-derived growth
factor receptor this insert region contains two SH2 binding
sites (26). Tyr-424 in RET/ptc2 corresponds to Y1158 in the
insulin receptor (26), and phosphorylation at Y1158 is required
for full activity (27). Tyr-505 is in a sequence that aligns with

the H-helix of the insulin receptor tyrosine kinase (18, 28). This
tyrosine is highly conserved in the receptor tyrosine kinases
(26) and could serve a structural role rather than as an SH2
docking site. Tyr-586, which completely eliminated mitogenic
activity when mutated to Phe, is in the carboxyl-terminal tail of
the RET$_{tk}$.

Tyrosines 586 and 350 are the best candidates for residues
that provide SH2 or phosphotyrosine binding domain docking
sites essential for the mitogenic response of RET/ptc2. Muta-
tion of the other Tyr in the COOH-terminal tail, Tyr-553, had
no effect on mitogenic activity. Results from the Y586F mutant
indicate that kinase activity alone is not sufficient for the
mitogenic response of RET/ptc2. Work is under way to investi-
gate RET/ptc2 phosphorylation sites and to search for interact-
ing proteins.

REFERENCES

1. Takahashi, M., Ritz, J., and Cooper, G. M. (1985) *Cell* 42, 581–588
2. Takahashi, M., Buma, Y., and Hiai, H. (1989) *Oncogene* 4, 805–806
3. Romeo, G., Ronchetto, P. Luo, Y., Barone, V., Seri, M., Ceccherini, I., Pasini,
   B., Bocciardi, R., Lerone, M., Kaariainen, H., and Martucciello, G. (1994)
   Nature 367, 377–378
4. Edery, P., Lyonnet, S., Mulligan, L., Pelet, A., Dow, E., Abel, L., Holder, S.,
   Nihoul-Fekete, C., Ponder, B., and Munnich, A. (1994) *Nature* 367, 378–380
5. Mulligan, L., Eng, C., Healey, C., Clayton, D., Kwok, J., Gardner, E., Ponder,
   M., Frilling, A., Jackson, C., Lehnert, H., Neumann, H., Thibodeau, S., and
   Ponder, B. (1994) *Nat. Genet.* 6, 70–74
6. Eng, C., Smith, D., Mulligan, L., Nagai, M., Healey, C., Ponder, M., Gardner,
   E., Scheumann, G., Jackson, C., Tunnacliffe, A., and Ponder, B. (1994)
   Hum. Mol. Genet. 3, 237–241
7. Hofstra, R., Landsvater, R., Ceccherini, I., Stulp, R., Stelwagen, T., Luo, Y.,
   Pasini, B., Hoppener, J., van Amstel, H., Romeo, G., Lips, C., and Buys, C.
   (1994) *Nature* 367, 375–376
8. Santoro, M., Carlomagno, F., Romano, A., Bottaro, D., Dathan, N., Grieco, M.,
   Fusco, A., Vecchio, G., Matoskova, B., Kraus, M., and Di Fiore, P. (1995)
   Science 267, 381–383
9. Bongarzone, I., Butti M., Coronelli, S., Borrello, M., Santoro, M., Mondellini,
   P., Pilotti, S., Fusco, A., Della Porta, G., and Pierotti, M. (1994) *Cancer Res.*
   54, 2979–2985
10. Lanzi, C., Borrello, M., Bongarzone, I., Migliazza, A., Fusco, A., Grieco, M.,
    Santoro, M., Gambetta, R., Zunino, F., Della Porta, G., and Pierotti, M.
    (1992) *Oncogene* 7, 2189–2194
11. Bongarzone, I., Monzini, N., Borrello, M., Carcano, C., Ferraresi, G., Arighi, E.,
    Mondellini, P., Della Porta, G., and Pierotti, M. (1993) *Mol. Cell Biol.* 13,
    358–366
12. Bubis, J., Vedvick, T., and Taylor, S. (1987) *J. Biol. Chem.* 262, 14961–14966
13. Sanger, F., Nicklen, S., and Coulson, A. R. (1977) *Proc. Natl. Acad. Sci. U. S. A.*
    74, 5463–5467
14. Kunkle, T. A., Bebenek, K., and McClary, J. (1991) *Methods Enzymol.* 204,
    125–139
15. Ausubel, F., Brent, R., Kingston, R., Moore, D., Seidman, J., Smith, J., and
    Struhl, K. (1994) *Current Protocols in Molecular Biology,* John Wiley &
    Sons, Inc., Brooklyn, NY
16. Meinkoth, J., Goldsmith, P., Spiegel, A., Feramisco, J., and Burrow, G. (1992)
    J. Biol. Chem. 267, 13239–13245
17. Bubis, J., Neitzel, J., Saraswat, L., and Taylor, S. (1988) *J. Biol. Chem.* 263,
    9668–9673
18. Hanks, S. K., Quinn, A. M., and Hunter, T. (1988) *Science* 241, 42–52
19. Pasini, B., Borrello, M., Greco, A., Bongarzone, I., Luo, Y., Mondellini, P.,
    Alberti, L., Miranda, C., Arighi, E., Bocciardi, R., Seri, M., Barone, V.,
    Romeo, G., and Pierotti, M. (1995) *Nat. Genet.* 10, 35–40
20. Taylor, S., Buechler, J., and Yonemoto, W. (1990) *Annu. Rev. Biochem.* 59,
    971–1005
21. Ullrich, A., and Schlessinger, J. (1990) *Cell* 61, 203–212
22. Schlessinger, J. (1988) *Trends Biochem. Sci.* 13, 443–447
23. Koch, C., Anderson, A., Moran, M., Ellis, C., and Pawson, T. (1991) *Science*
    252, 668–674
24. Wells, A., Welsh, J., Lazar, C., Wiley, H., Gill, G., and Rosenfeld, M. (1990)
    Science 247, 962–964
25. Reddy, C., Wells, A., and Lauffenburger, D. (1994) *Biotech. Prog.* 10, 377–384
26. van der Geer, P., Hunter, T., and Lindberg, R. (1994) *Annu. Rev. Cell Biol.* 10,
    251–337
27. White, M., Shoelson, S., Keutmann, H., and Kahn, C. (1988) *J. Biol. Chem.*
    263, 2969–2980
28. Hubbard, S., Wei, L., Ellis, L., and Hendrickson, W. (1994) *Nature* 372,
    746–754

Orig. Op.	OPERATOR:	PROOF:	PE's:	AA's:	COMMENTS:	ARTNO:
1st K35, 2nd	judy					352754